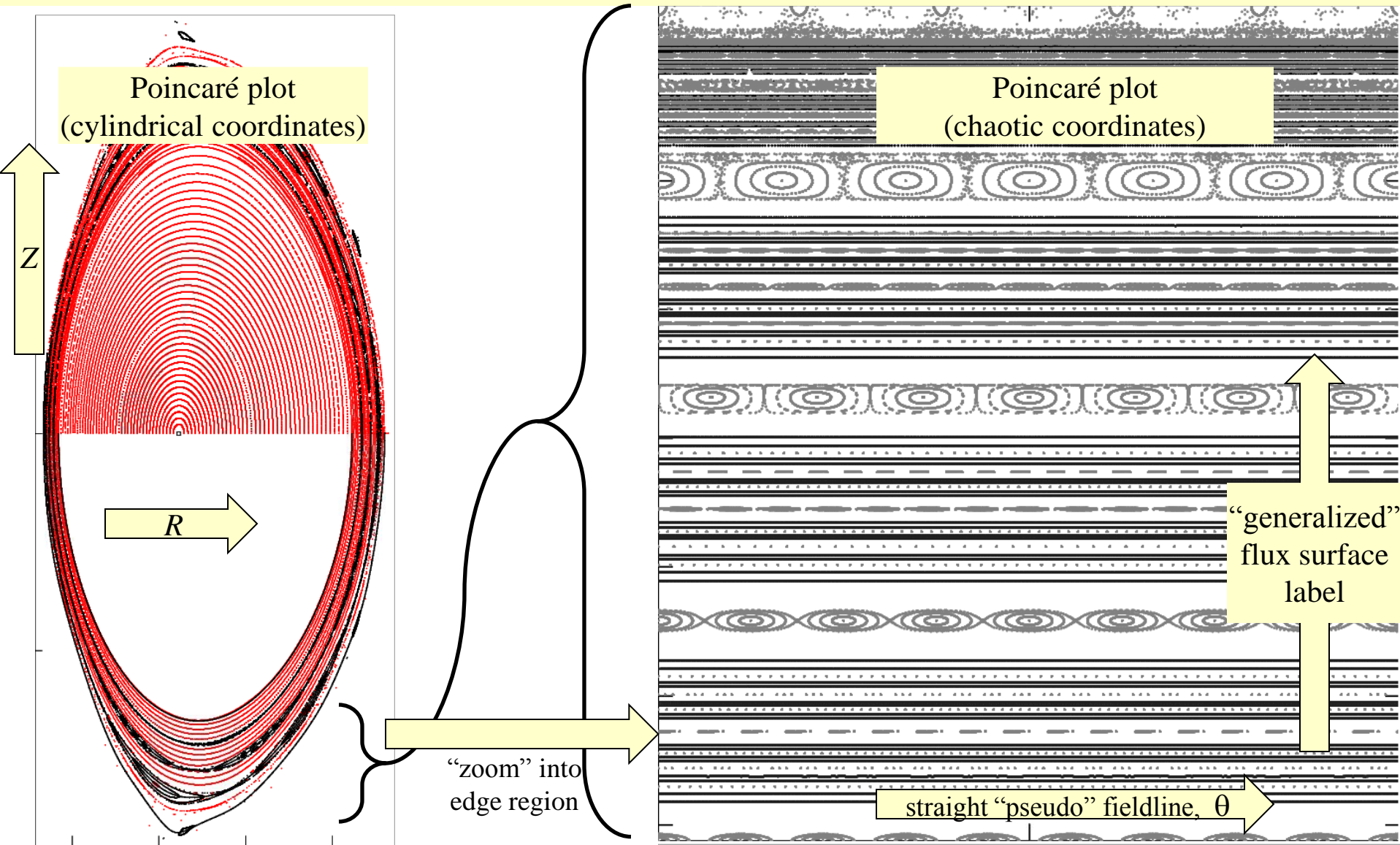


# Chaotic coordinates for LHD

S. R. Hudson, Y. Suzuki & R. L. Dewar.

Princeton Plasma Physics Laboratory, National Institute for Fusion Science, Australian National University.



Goal: a robust, *fast* construction of “magnetic” coordinates adapted to the invariant structures of non-integrable magnetic fields.

The geometry and chaotic structure of  $\mathbf{B}$  is fundamental:

- geometry (e.g. curvature, shear, ...) affects stability, confinement, . .
- chaotic structure (e.g. flux surfaces, chaotic fieldlines,) affects stability, confinement, . .

**NON-INTEGRABLE FIELDS ARE GENERIC;  
EXISTENCE OF ISLANDS & CHAOS AFFECTS ALL AREAS OF PLASMA CONFINEMENT !**

Straight fieldline coordinates

(i) are extremely useful, and

(ii) *can* be constructed on the invariant sets

(this includes the “rational” periodic fieldlines, and the “irrational” KAM surfaces & cantori).

“Chaotic coordinates” are based on a selection of “almost-invariant” quadratic-flux minimizing (QFM) surfaces.

→ QFM surfaces pass through the islands and “capture” the remnant invariant sets.

The fractal structure of  $\mathbf{B}$  is absorbed into the coordinates;

→ the flux surfaces are straight and the islands are “square”.

# Mathematical Preliminary: Toroidal Coordinates

The magnetic field is usually given in cylindrical coordinates; arbitrary, toroidal coordinates are introduced.

- “Inverse” coordinate transformation from  $(\rho, \theta, \zeta)$  to  $(R, \phi, Z)$ :

$$R \equiv \sum_{m,n} R_{m,n}(\rho) \cos(m\theta - n\zeta), \quad \phi \equiv \zeta, \quad Z \equiv \sum_{m,n} Z_{m,n}(\rho) \sin(m\theta - n\zeta).$$

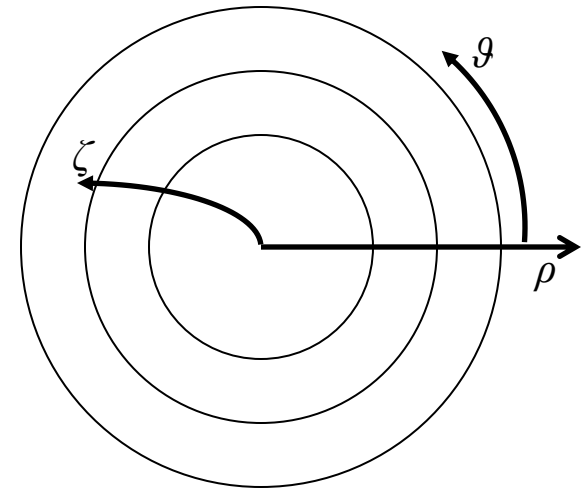
- The Fourier harmonics,  $R_{m,n}(\rho_i)$  &  $Z_{m,n}(\rho_i)$ , of a discrete set of “coordinate surfaces” are interpolated and extrapolated using cubic/quintic polynomials; this works if the surfaces are smooth and well separated; a regularization factor,  $\rho^{m/2}$ , is included near origin.

- Any coordinate transformation defines a vector transformation,

$$\begin{pmatrix} B^R \\ B^\phi \\ B^Z \end{pmatrix} = \begin{pmatrix} R_\rho & R_\theta & R_\zeta \\ \phi_\rho & \phi_\theta & \phi_\zeta \\ Z_\rho & Z_\theta & Z_\zeta \end{pmatrix} \begin{pmatrix} B^\rho \\ B^\theta \\ B^\zeta \end{pmatrix}.$$

- The construction of chaotic-coordinates is iterative:

1. begin with a discrete set of (e.g. circular cross-section) surfaces that define approximate flux coordinates; coordinate origin = magnetic axis, which is found iteratively;
2. construct a set of QFM surfaces  $\equiv$  *pseudo* flux surfaces;
3. Fourier decompose each QFM surface in a straight *pseudo* fieldline angle;
4. replace coordinate surfaces with QFM surfaces;
5. include additional QFM surfaces; construct a hierarchy of chaotic coordinates.



# Mathematical Preliminary: Vector Potential

A magnetic vector potential, in a suitable gauge, is quickly determined by radial integration.

1. Generally, gauge freedom allows  $\mathbf{A} = A_\theta(\rho, \theta, \zeta)\nabla\theta + A_\zeta(\rho, \theta, \zeta)\nabla\zeta$ .

2.  $\nabla \times \mathbf{B} = \mathbf{A}$  gives

$$\begin{aligned}\sqrt{g}B^\rho &= \partial_\theta A_\zeta - \partial_\zeta A_\theta, \\ \sqrt{g}B^\theta &= -\partial_\rho A_\zeta, \\ \sqrt{g}B^\zeta &= \partial_\rho A_\theta.\end{aligned}$$

3. Given the magnetic field,  $\mathbf{A}$  is quickly determined by radial integration in Fourier space:

$$\begin{aligned}\partial_\rho A_{\theta,m,n} &= +(\sqrt{g}B^\zeta)_{m,n}, \\ \partial_\rho A_{\zeta,m,n} &= -(\sqrt{g}B^\theta)_{m,n},\end{aligned}$$

and the remaining equation,  $\sqrt{g}B^\rho = \partial_\theta A_\zeta - \partial_\zeta A_\theta$ , is satisfied if  $\nabla \cdot \mathbf{B} = 0$ .

4. Hereafter, use notation  $\mathbf{A} = \psi\nabla\theta - \chi\nabla\zeta$ .

# Magnetic flux surfaces are required for good confinement; but 3D effects create “magnetic islands”, and island overlap creates chaos.

1.  $\mathbf{A} = \psi(\rho, \theta, \zeta) \nabla \theta - \chi(\rho, \theta, \zeta) \nabla \zeta = \psi \nabla \theta - \chi(\psi, \theta, \zeta) \nabla \zeta$ ,  $\underbrace{\text{if } \rho \equiv \rho(\psi, \theta, \zeta)}_{\text{coordinate transformation}}$
2.  $\mathbf{B} = \nabla \psi \times \nabla \theta - \nabla \chi(\psi, \theta, \zeta) \times \nabla \zeta$
3. Toroidal flux:  $\int_{\mathcal{S}} \mathbf{B} \cdot d\mathbf{s} = \int_0^{2\pi} d\theta \int_0^{\psi} d\bar{\psi} \mathbf{B} \cdot \mathbf{e}_{\psi} \times \mathbf{e}_{\theta} = 2\pi\psi$ , where  $\sqrt{g} \equiv \mathbf{e}_{\psi} \cdot \mathbf{e}_{\theta} \times \mathbf{e}_{\zeta} = (\nabla \psi \cdot \nabla \theta \times \nabla \zeta)^{-1}$ .
4. Definition of fieldline:  $d\mathbf{l} \propto \mathbf{B}$ .

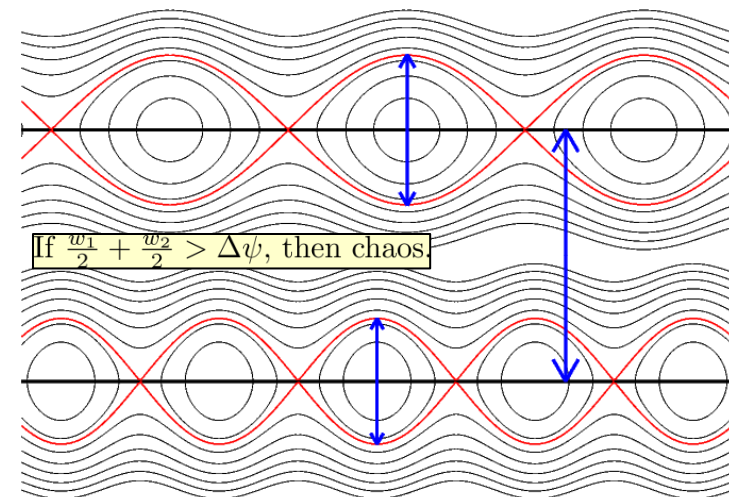
- Cartesian  $(x, y, z)$  coordinate basis:  $dx \mathbf{i} + dy \mathbf{j} + dz \mathbf{k} = B^x \mathbf{i} + B^y \mathbf{j} + B^z \mathbf{k}$ .
- Arbitrary  $(\psi, \theta, \zeta)$  coordinate basis:  $d\psi \mathbf{e}_{\psi} + d\theta \mathbf{e}_{\theta} + d\zeta \mathbf{e}_{\zeta} = B^{\psi} \mathbf{e}_{\psi} + B^{\theta} \mathbf{e}_{\theta} + B^{\zeta} \mathbf{e}_{\zeta}$ , where  $B^{\psi} \equiv \mathbf{B} \cdot \nabla \psi$ ,  $B^{\theta} \equiv \mathbf{B} \cdot \nabla \theta$ ,  $B^{\zeta} \equiv \mathbf{B} \cdot \nabla \zeta$ .

$$5. \quad \dot{\psi} \equiv \frac{d\psi}{d\zeta} = \frac{B^{\psi}}{B^{\zeta}} = -\frac{\partial \chi}{\partial \theta}, \quad \dot{\theta} \equiv \frac{d\theta}{d\zeta} = \frac{B^{\theta}}{B^{\zeta}} = \frac{\partial \chi}{\partial \psi};$$

$\chi \equiv \text{poloidal flux} \equiv \text{fieldline Hamiltonian}.$

6. If  $\chi = \chi(\psi)$ ,  $\dot{\psi} = 0$  and  $\dot{\theta} = \iota(\psi)$ : magnetic field is “integrable”, and fieldlines lie on nested flux surfaces.

7. Generally,  $\chi = \chi(\psi, \theta, \zeta) = \sum_{m,n} \chi_{m,n}(\psi) \cos(m\theta - n\zeta)$ , and “islands” open where  $m\dot{\theta} - n = 0$ .



# Physics Preliminary: Magnetic Fieldline Action

The action is the line integral, along an arbitrary curve, of the vector potential.

$S[\mathcal{C}] \equiv \int_{\mathcal{C}} \mathbf{A} \cdot d\mathbf{l}$ , along trial curve,  $\mathcal{C} : \rho = \rho(\zeta), \theta = \theta(\zeta)$ .

$\mathbf{A} = \psi \nabla \theta - \chi \nabla \zeta$ ,  $d\mathbf{l} \equiv d\rho e_\rho + d\theta e_\theta + d\zeta e_\zeta$ ,  $\mathbf{A} \cdot d\mathbf{l} = (\psi \dot{\theta} - \chi) d\zeta$ .

e.g.  $\psi = \sum_{m,n} \psi_{m,n}(\rho) \cos(m\theta - n\zeta)$ ,  $\chi = \sum_{m,n} \chi_{m,n}(\rho) \cos(m\theta - n\zeta)$ .

Numerically, a curve is represented as piecewise-constant, piecewise-linear.

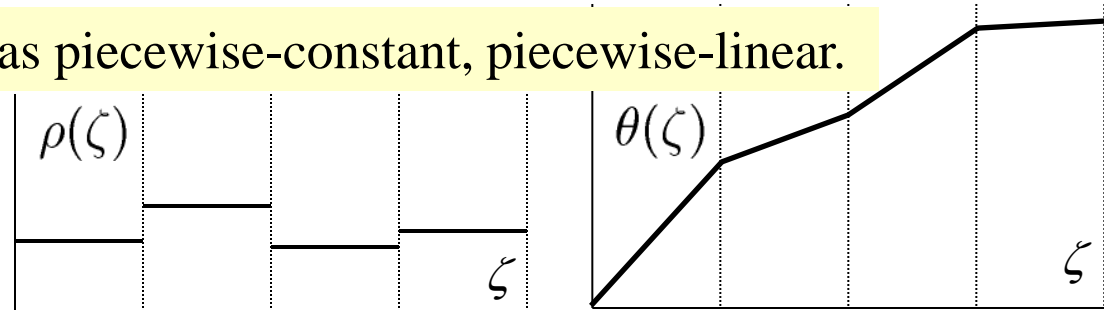
For  $\zeta \in (\zeta_{i-1}, \zeta_i)$ ,

$\rho(\zeta) = \rho_i$ ,

$\theta(\zeta) = \theta_{i-1} + \dot{\theta} (\zeta - \zeta_{i-1})$ ,

where  $\dot{\theta} \equiv (\theta_i - \theta_{i-1}) / \Delta\zeta$ .

The  $\{\rho_i : i = 1, N\}$  and  $\{\theta_i : i = 0, N\}$  describe the curve.  $N$  is resolution. Periodicity:  $\zeta_N = 2\pi q$ ,  $\theta_N = \theta_0 + 2\pi p$ .



Seems crude; but, the trigonometric integrals are computed analytically, i.e. *fast*;

$$S = \sum_{i=1}^N \int_{\zeta_{i-1}}^{\zeta_i} d\zeta (\psi \dot{\theta} - \chi) = \sum_{i=1}^N \sum_{m,n} [\psi_{m,n}(\rho_i) \dot{\theta} - \chi_{m,n}(\rho_i)] \int_{\zeta_{i-1}}^{\zeta_i} d\zeta \cos(m\theta - n\zeta)$$

$$\int_{\zeta_{i-1}}^{\zeta_i} d\zeta \cos(m\theta - n\zeta) = \frac{\sin(m\theta_i - n\zeta_i) - \sin(m\theta_{i-1} - n\zeta_{i-1})}{m\dot{\theta} - n}$$

and, coordinates will be constructed in which the periodic fieldlines are straight.

# The construction of extremal *curves* of the *action* can be generalized to the construction of extremizing *surfaces* of the *quadratic-flux*.

1.  $\delta S = \int_c d\zeta \left( \delta\theta \frac{\partial S}{\partial\theta} + \delta\rho \frac{\partial S}{\partial\rho} \right)$ , where  $\frac{\partial S}{\partial\theta} \equiv \sqrt{g}B^\rho - \dot{\rho}\sqrt{g}B^\zeta$  and  $\frac{\partial S}{\partial\rho} \equiv \dot{\theta}\sqrt{g}B^\zeta - \sqrt{g}B^\theta$ .
2. Extremal curves satisfy  $\frac{\partial S}{\partial\theta} = 0$ , i.e.  $\dot{\rho} = B^\rho/B^\zeta$ , and  $\frac{\partial S}{\partial\rho} = 0$ , i.e.  $\dot{\theta} = B^\theta/B^\zeta$ .
3. Introduce toroidal surface,  $\rho \equiv P(\theta, \zeta)$ , and *family* of angle curves,  $\theta_\alpha(\zeta) \equiv \alpha + p\zeta/q + \tilde{\theta}(\zeta)$ , where  $\alpha$  is a fieldline label;  $p$  and  $q$  are integers that determine periodicity; and  $\tilde{\theta}(0) = \tilde{\theta}(2\pi q) = 0$ .
4. On *each* curve,  $\rho_\alpha(\zeta) = P(\theta_\alpha(\zeta), \zeta)$  and  $\theta_\alpha(\zeta)$ , can enforce  $\frac{\partial S}{\partial\rho} = 0$ ; generally  $\nu \equiv \frac{\partial S}{\partial\theta} \neq 0$ .
5. The *pseudo* surface dynamics is defined by  $\dot{\theta} \equiv B^\theta/B^\zeta$  and  $\dot{\rho} \equiv \partial_\theta P \dot{\theta} + \partial_\zeta P$ .
6. Corresponding *pseudo* field  $\mathbf{B}_\nu \equiv \dot{\rho} B^\zeta \mathbf{e}_\rho + \dot{\theta} B^\zeta \mathbf{e}_\theta + B^\zeta \mathbf{e}_\zeta$ ; simplifies to  $\mathbf{B}_\nu = \mathbf{B} - \frac{\nu}{\sqrt{g}} \mathbf{e}_\rho$ .
7. Introduce the quadratic-flux functional:  $\varphi_2 \equiv \frac{1}{2} \iint d\theta d\zeta \left( \frac{\partial S}{\partial\theta} \right)^2$
8. Allowing for  $\delta P$ , the first variation is  $\delta\varphi_2 = \iint d\theta d\zeta \delta P \sqrt{g} (B^\theta \partial_\theta + B^\zeta \partial_\zeta) \nu$ .

# The action gradient, $\nu$ , is constant along the pseudo fieldlines; construct Quadratic Flux Minimizing (QFM) surfaces by *pseudo* fieldline (local) integration.

1. The *true* fieldline flow along  $\mathbf{B}$  around  $q$  toroidal periods from  $(\theta_0, \rho_0)$  produces a mapping, 
$$\begin{pmatrix} \theta_q \\ \rho_q \end{pmatrix} = M^q \begin{pmatrix} \theta_0 \\ \rho_0 \end{pmatrix}.$$
2. Periodic fieldlines are fixed points of  $M^q$ , i.e.  $\theta_q = \theta_0 + 2\pi p$ ,  $\rho_q = \rho_0$ .
3. In integrable case: given  $\theta_0$ , a one-dimensional search in  $\rho$  is required to find the *true* periodic fieldline.
4. In non-integrable case, only the
  - (i) “stable” (action-minimax),  $O$ , (which is not always stable), and the
  - (ii) unstable (action minimizing),  $X$ , periodic fieldlines are guaranteed to survive.
5. The *pseudo* fieldline flow along  $\mathbf{B}_\nu = \mathbf{B} - \frac{\nu}{\sqrt{g}} \mathbf{e}_\rho$  around  $q$  periods from  $(\theta_0, \rho_0)$  produces a mapping, 
$$\begin{pmatrix} \theta_q \\ \rho_q \end{pmatrix} = P^q \begin{pmatrix} \nu \\ \rho_0 \end{pmatrix},$$
 but  $\nu$  is not yet known.
6. In general case: given  $\theta_0$ , a two-dimensional search in  $(\nu, \rho)$  is required to find the periodic *pseudo* fieldline.



# Alternative Lagrangian integration construction: QFM surfaces are families of extremal curves of the constrained-area action integral.

1. Introduce  $F(\boldsymbol{\rho}, \boldsymbol{\theta}) \equiv \int_{\mathcal{C}} \mathbf{A} \cdot d\mathbf{l} - \nu \left( \int_{\mathcal{C}} \theta \nabla \zeta \cdot d\mathbf{l} - a \right)$ , where  $\boldsymbol{\rho} \equiv \{\rho_i\}$ ,  $\boldsymbol{\theta} \equiv \{\theta_i\}$ ;

where  $\nu$  is a Lagrange multiplier, and  $a$  is the required “area”,  $\int_0^{2\pi q} \theta(\zeta) d\zeta$ .

2. An identity of vector calculus gives  $\delta F = \int_{\mathcal{C}} d\mathbf{l} \times (\nabla \times \mathbf{A} - \nu \nabla \theta \times \nabla \zeta) \cdot \delta \mathbf{l}$ ,

extremizing curves are tangential to  $\mathbf{B} - \nu \nabla \theta \times \nabla \zeta = \mathbf{B} - \frac{\nu}{\sqrt{g}} \mathbf{e}_\rho = \mathbf{B}_\nu$ .

3. Constrained-area action-extremizing curves satisfy  $\frac{\partial F}{\partial \rho_i} = 0$  and  $\frac{\partial F}{\partial \theta_i} = 0$ .

4. The piecewise-constant representation for  $\rho(\zeta)$  and  $\partial_{\rho_i} F = 0$  yields  $\rho_i = \rho_i(\theta_{i-1}, \theta_i)$ , so the trial curve is completely described by  $\theta_i$ , i.e.  $F \equiv F(\boldsymbol{\theta})$ .

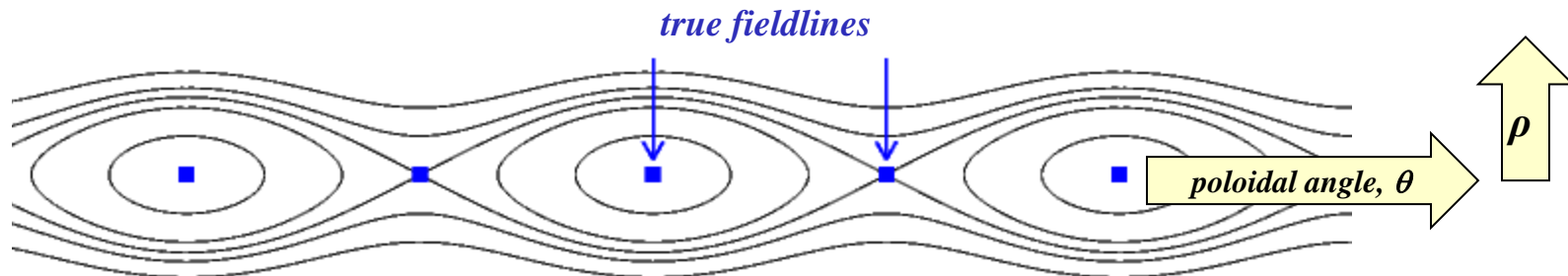
5. The piecewise-linear representation for  $\theta(\zeta)$  gives  $\frac{\partial F}{\partial \theta_i} = \partial_2 F_i(\theta_{i-1}, \theta_i) + \partial_1 F_{i+1}(\theta_i, \theta_{i+1})$ , so the Hessian,  $\nabla^2 F(\boldsymbol{\theta})$ , is tridiagonal (assuming  $\nu$  is given) and is easily inverted.

6. Multi-dimensional Newton method:  $\delta \boldsymbol{\theta} = - (\nabla^2 F)^{-1} \cdot \nabla F(\boldsymbol{\theta})$ ;

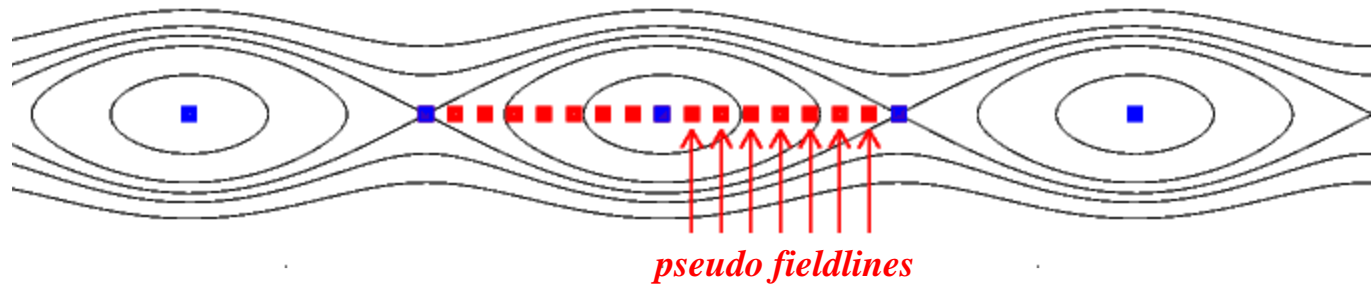
*global* integration, much less sensitive to “Lyapunov” integration errors.

At each poloidal angle, compute radial “*error*” field that must be subtracted from  $\mathbf{B}$  to create a periodic curve, and so create a rational, *pseudo* flux surface.

0. Usually, there are only the “stable” periodic fieldline and the unstable periodic fieldline,

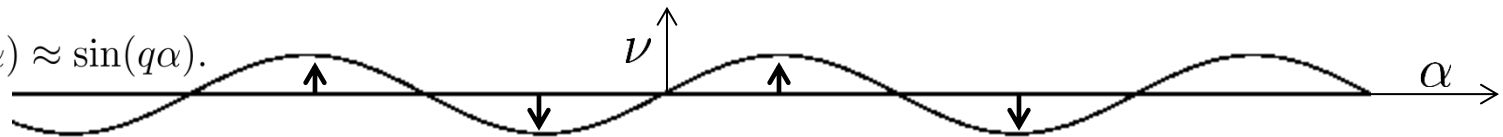


1. At every  $\theta = \alpha$ , determine  $\nu(\alpha)$  via numerical search so that  $\mathbf{B} - \nu \mathbf{e}_\rho / \sqrt{g}$  yields a periodic integral curve; where  $\alpha$  is a fieldline label.



2. At the true periodic fieldlines, the required additional radial field is zero: i.e.  $\nu(\alpha_0) = 0$  and  $\nu(\alpha_X) = 0$ .

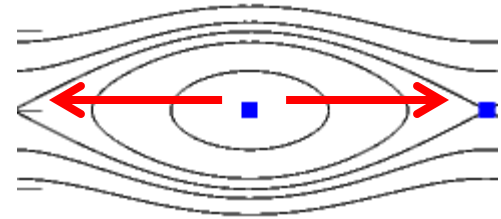
3. Typically,  $\nu(\alpha) \approx \sin(q\alpha)$ .



4. The pseudo fieldlines “capture” the true fieldlines; QFM surfaces pass through the islands.

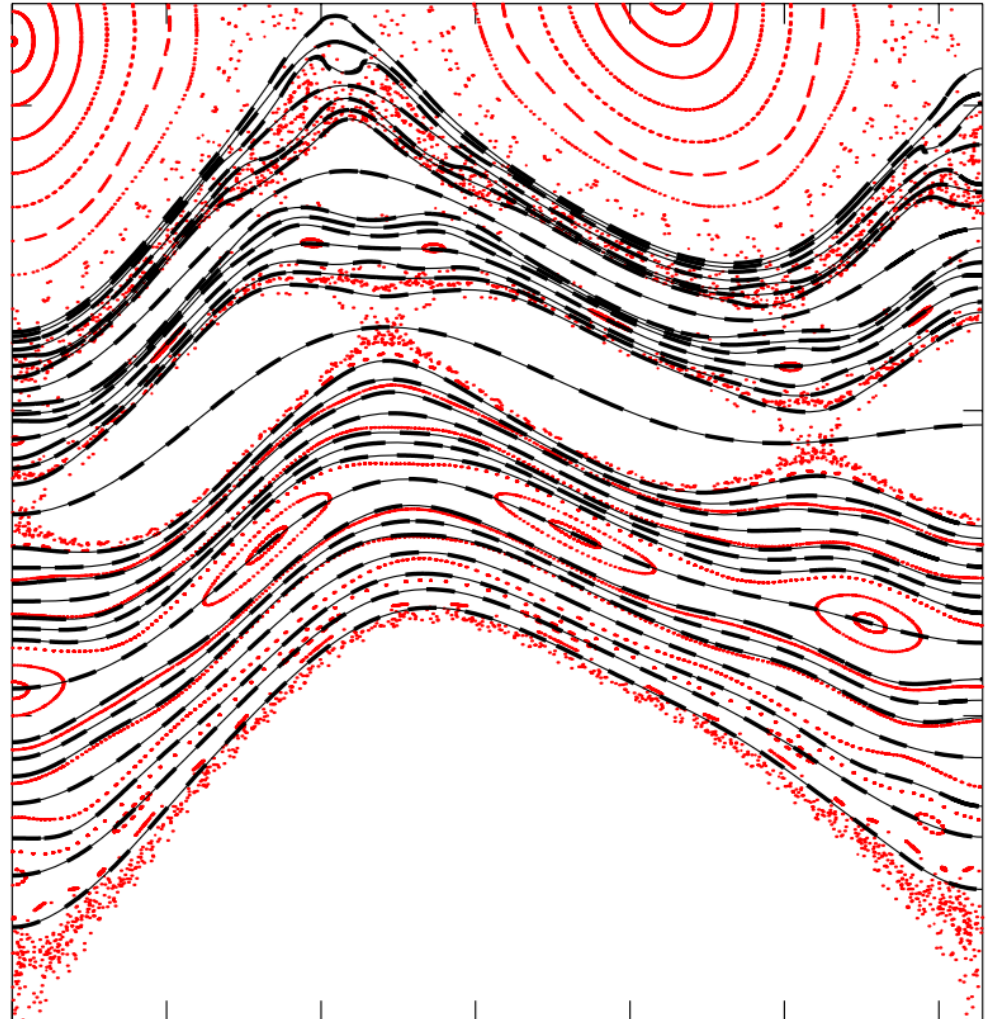
# Ghost surfaces, another class of almost-invariant surface, are defined by an action-gradient flow between the action minimax and minimizing fieldline.

1. Action,  $S[\mathcal{C}] \equiv \int_{\mathcal{C}} \mathbf{A} \cdot d\mathbf{l}$ , and action gradient,  $\frac{\partial S}{\partial \theta} \equiv \sqrt{g}B^\rho - \dot{\rho}B^\zeta$ .
2. Enforce  $\frac{\partial S}{\partial \rho} \equiv \dot{\theta}B^\zeta - \sqrt{g}B^\theta = 0$ , i.e. invert  $\dot{\theta} \equiv B^\theta/B^\zeta$  to obtain  $\rho = \rho(\dot{\theta}, \theta, \zeta)$ ; so that trial curve is completely described by  $\theta(\zeta)$ , and the action reduces from  $S \equiv S[\rho(\zeta), \theta(\zeta)]$  to  $S \equiv S[\theta(\zeta)]$
3. Define action-gradient flow:  $\frac{\partial \theta(\zeta; \tau)}{\partial \tau} \equiv -\frac{\partial S[\theta]}{\partial \theta}$ , where  $\tau$  is an arbitrary integration parameter.
4. Ghost-surfaces are constructed as follows:
  - Begin at action-minimax (“O”, “not-always-stable”) periodic fieldline, which is a saddle;
  - initialize integration in decreasing direction (given by negative eigenvalue/vector of Hessian);
  - the entire curve “flows” down the action gradient,  $\partial_\tau \theta = -\partial_\theta S$ ;
  - action is decreasing,  $\partial_\tau S < 0$ ;
  - finish at action-minimizing (“X”, unstable) periodic fieldline.
  - ghost surface described by  $\mathbf{x}(\zeta, \tau)$ , where  $\tau$  is a fieldline label.



# Ghost surfaces are (almost) indistinguishable from QFM surfaces; can redefine poloidal angle (straight pseudo fieldline) to unify ghost surfaces with QFMs.

1. Ghost-surfaces are defined by an (action gradient) flow.
2. QFM surfaces are defined by minimizing  $\int (\text{action gradient})^2 ds$ .
3. Not obvious if the different definitions give the same surfaces.
4. For model chaotic field:
  - (a) ghosts = thin solid lines;
  - (b) QFMs = thick dashed lines;
  - (c) agreement is excellent;
  - (d) difference =  $\mathcal{O}(\epsilon^2)$ , where  $\epsilon$  is perturbation.
5. Can redefine  $\theta$  to obtain unified theory of ghosts & QFMs; straight *pseudo* fieldline angle.



# Isotherms of the steady state solution to the anisotropic diffusion coincide with ghost surfaces; analytic, 1-D solution is possible.

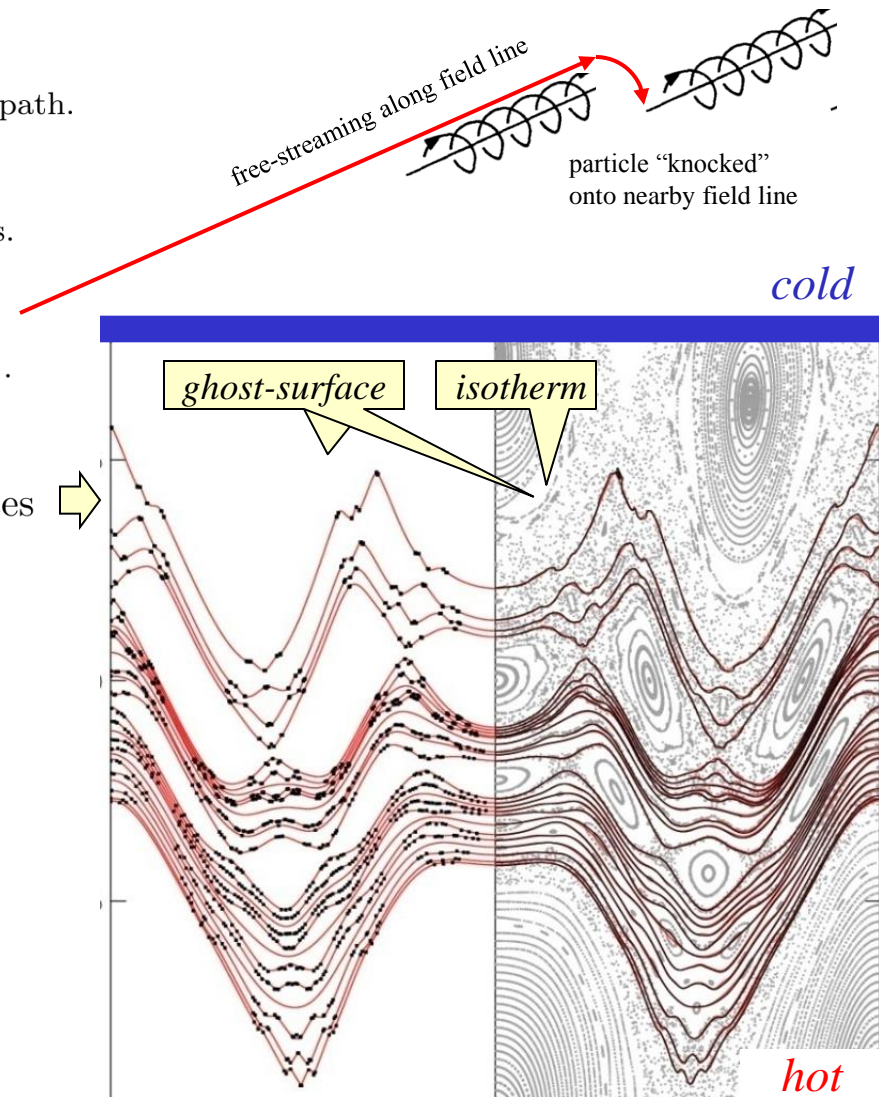
1. Transport along the magnetic field is unrestricted:  
e.g. parallel random walk with long steps  $\approx$  collisional mean free path.
2. Transport across the magnetic field is very small:  
e.g. perpendicular random walk with short steps  $\approx$  Larmor radius.
3. Simple transport model: anisotropic diffusion,  

$$\kappa_{\parallel} \nabla_{\parallel}^2 T + \kappa_{\perp} \nabla_{\perp}^2 T = 0, \quad \kappa_{\perp} / \kappa_{\parallel} \sim 10^{-10}, \text{ grid} = 2^{12} \times 2^{12}.$$
 steady state, no source, inhomogeneous boundary conditions.

4. Compare numerical solution to “irrational” ghost-surfaces  $\Rightarrow$
5. The temperature adapts to KAM surfaces, cantori, **and ghost-surfaces!**, i.e.  $T = T(\rho)$ .
6. From  $T = T(\rho, \theta, \zeta)$  to  $T = T(\rho)$  allows an expression for the temperature gradient in chaotic fields:

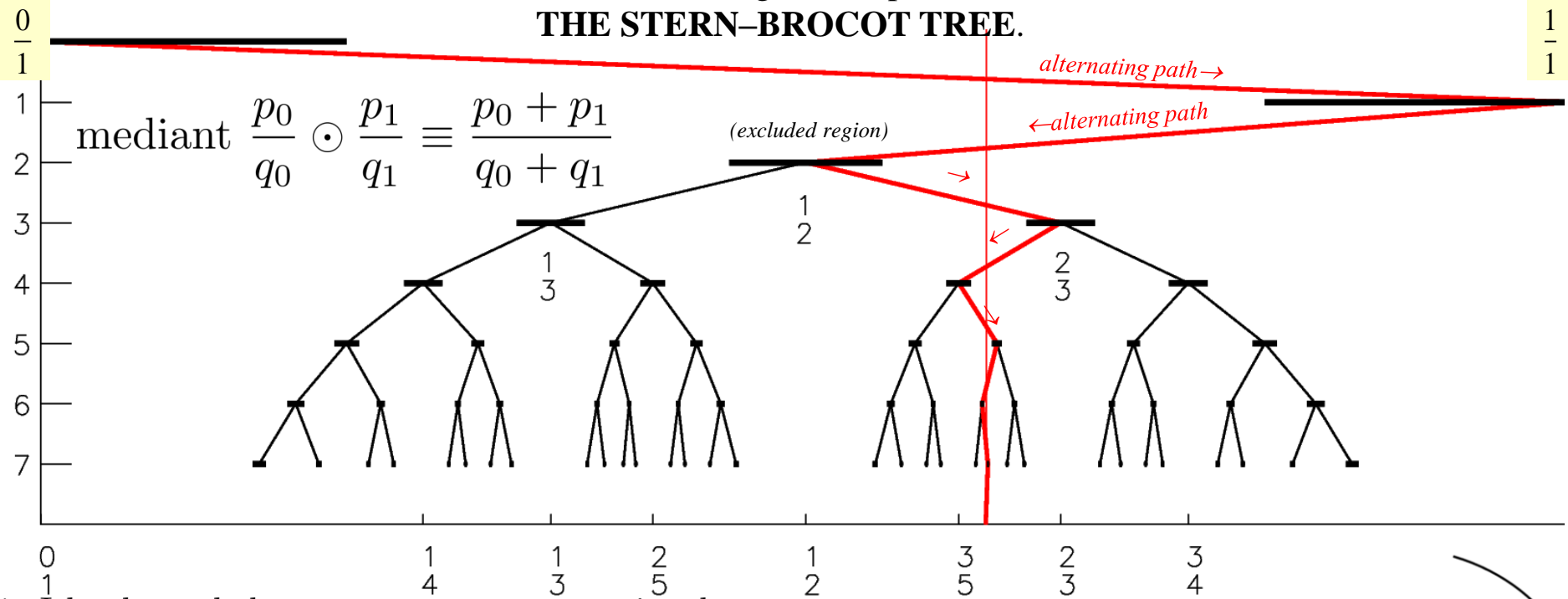
$$\frac{dT}{d\rho} \propto \frac{1}{\kappa_{\parallel} \varphi_2 + \kappa_{\perp} G},$$

where  $\varphi_2 \equiv \underbrace{\int B_n^2 ds}_{\text{quadratic flux}}$ , and  $G \equiv \underbrace{\int \nabla \rho \cdot \nabla \rho ds}_{\text{metric}}$ .



# Chaos Preliminary: The fractal structure of chaos is related to the structure of rationals and irrationals.

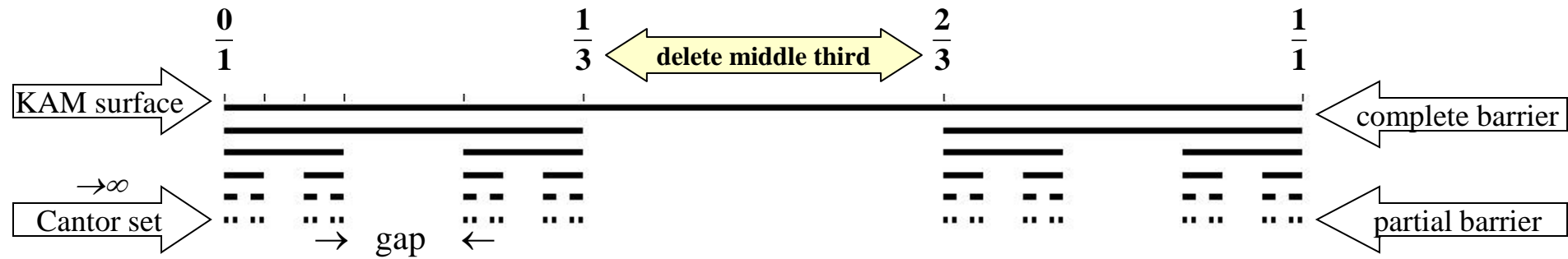
## THE FAREY TREE; or, according to Wikipedia, THE STERN-BROCOT TREE.



1. Islands, and chaos, emerge at every rational:  
about each rational,  $n/m$ , introduce “excluded region” with width  $r/m^k$ ; if excluded regions don't overlap, then
2. KAM theorem: irrational flux surface can survive if  $\underbrace{|\epsilon - n/m|}_{\text{Diophantine condition}} > r/m^k$  for all  $n, m$ .  
Call  $\epsilon$  *strongly irrational*.
3. Greene’s residue criterion: the most robust flux surfaces have “noble” transform:  
noble irrationals  $\equiv$  limit of ultimately alternating paths  $\equiv$  limit of Fibonacci ratios;  
e.g.  $\frac{0}{1}, \frac{1}{0}, \frac{1}{1}, \frac{2}{1}, \frac{3}{2}, \frac{5}{3}, \frac{8}{5}, \frac{13}{8}, \frac{21}{13}, \frac{34}{21}, \frac{55}{34}, \dots \rightarrow \gamma \equiv \text{golden mean} \equiv \frac{(1+\sqrt{5})}{2}$ ; e.g.  $\frac{1}{0}, \frac{0}{1}, \frac{1}{1}, \frac{1}{2}, \frac{2}{3}, \frac{3}{5}, \frac{5}{8}, \frac{8}{13}, \frac{13}{21}, \frac{21}{34}, \dots \rightarrow \gamma^{-1}$ .

Irrational “KAM” surfaces break into cantori when perturbation exceeds critical value.

Both KAM surfaces and cantori restrict transport.



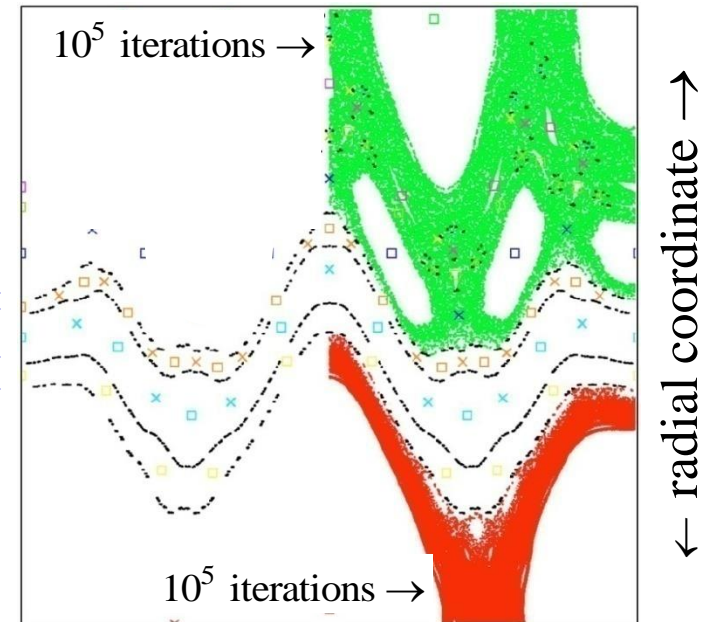
→ KAM surfaces are closed, toroidal surfaces that **stop** radial field line transport

→ Cantori have “gaps” that fieldlines can pass through; however, **cantori can severely restrict** radial transport

→ Example: all flux surfaces destroyed by chaos, but even after **100 000 transits** around torus the fieldlines **don’t get past cantori !**

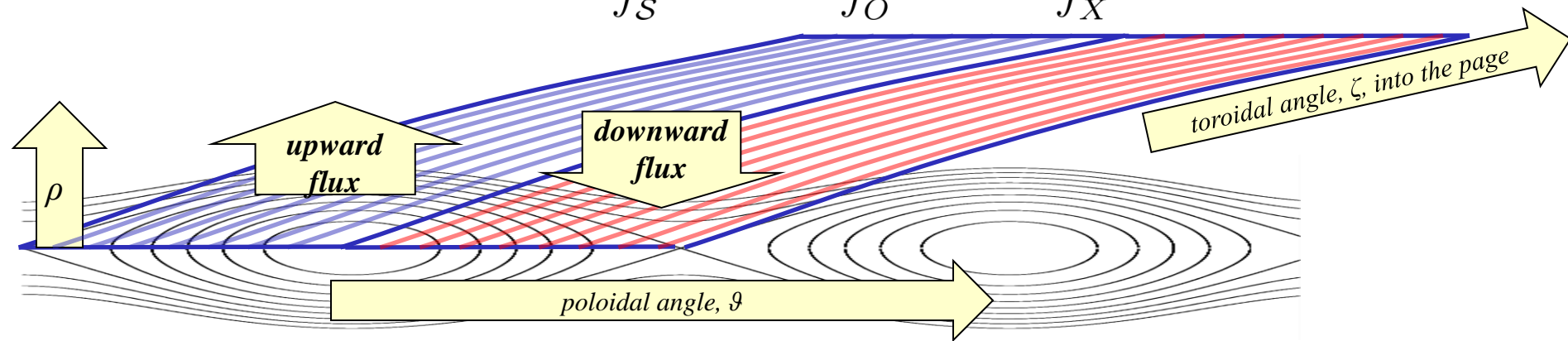
→ Regions of chaotic fields can provide some confinement because of the cantori partial barriers.

“noble”  
cantori  
(black dots)



The “upward” flux = “downward” flux across a toroidal surface passing through an island chain can be computed.

1.  $\int_{\partial\mathcal{V}} \mathbf{B} \cdot d\mathbf{S} = \int_{\mathcal{V}} \nabla \cdot \mathbf{B} = 0$ ; the total flux across any closed surface of  $\mathbf{B}$  is zero.
2. Consider “rational” surface with boundary coinciding with  $X$  and  $O$  fieldlines; define “upward” flux  $\Psi_{p/q} \equiv \int_S \mathbf{B} \cdot d\mathbf{S} = \int_O \mathbf{A} \cdot d\mathbf{l} - \int_X \mathbf{A} \cdot d\mathbf{l}$ .



1. Consider sequence of rationals that approach an irrational, i.e.  $p_i/q_i \rightarrow t$  as  $i \rightarrow \infty$ ,
  - if  $\Psi_{p_i/q_i} \rightarrow \Psi_t = 0$ , then  $\text{KAM}_t$  surface exists, a perfect barrier to transport;
  - if  $\Psi_{p_i/q_i} \rightarrow \Psi_t > 0$ , then  $\Psi_t$  quantifies flux across cantorus $_t$ , a “partial” barrier.
2.  $\Psi_{p/q}$  called “Mather’s difference in action”;  $\Psi_t$  quantifies strength of partial barrier.

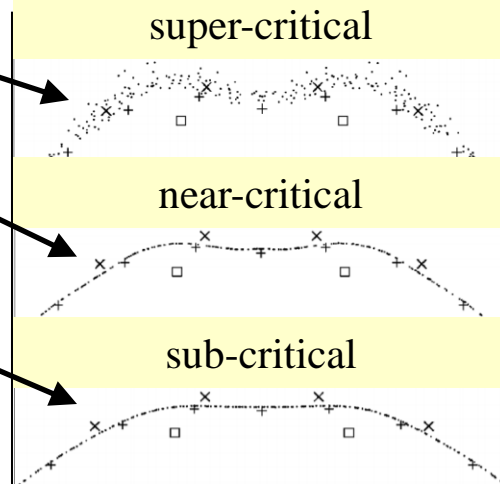
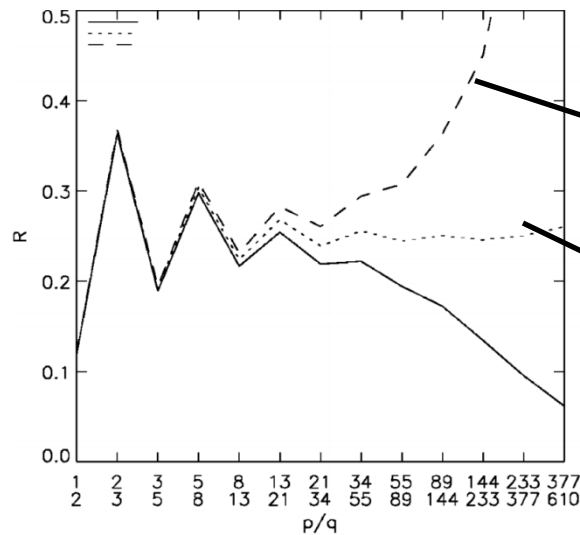


# Greene's residue criterion: the existence of an irrational flux surface is determined by the stability of closely-approximating periodic orbits.

1. The tangent map is defined  $\begin{pmatrix} \delta\theta_q \\ \delta\rho_q \end{pmatrix} = \nabla M^q \begin{pmatrix} \delta\theta_0 \\ \delta\rho_0 \end{pmatrix}$ .
2. The eigenvalues of  $\nabla M^q$  at periodic fieldlines determine stability:  $|\nabla M^q| = 1$ ;  $\lambda_1 = 1/\lambda_2$ ; if  $|\lambda| > 1$ , unstable, exponential; if  $|\lambda| = 1$ , stable, sinusoidal.
3. The residue is defined  $R_{p/q} \equiv (2 - \lambda - \lambda^{-1})/4$ .
4. Consider sequence of rationals that approach an irrational, i.e.  $p_i/q_i \rightarrow t$  as  $i \rightarrow \infty$ . (the "best" approximations called the convergents, given by continued fractions).

If  $R_{p/q} \rightarrow 0$ , surface<sub>t</sub> exists;  
 if  $R_{p/q} \rightarrow \frac{1}{4}$ , surface<sub>t</sub> critical; and  
 if  $R_{p/q} \rightarrow \infty$ , surface<sub>t</sub> destroyed.

5. By cleverly searching Farey tree [following Greene, MacKay] can find "boundary surface"  $\equiv$  last, closed, flux surface.



Large Helical Device (LHD):  
low order islands near edge  
create chaotic fieldlines.

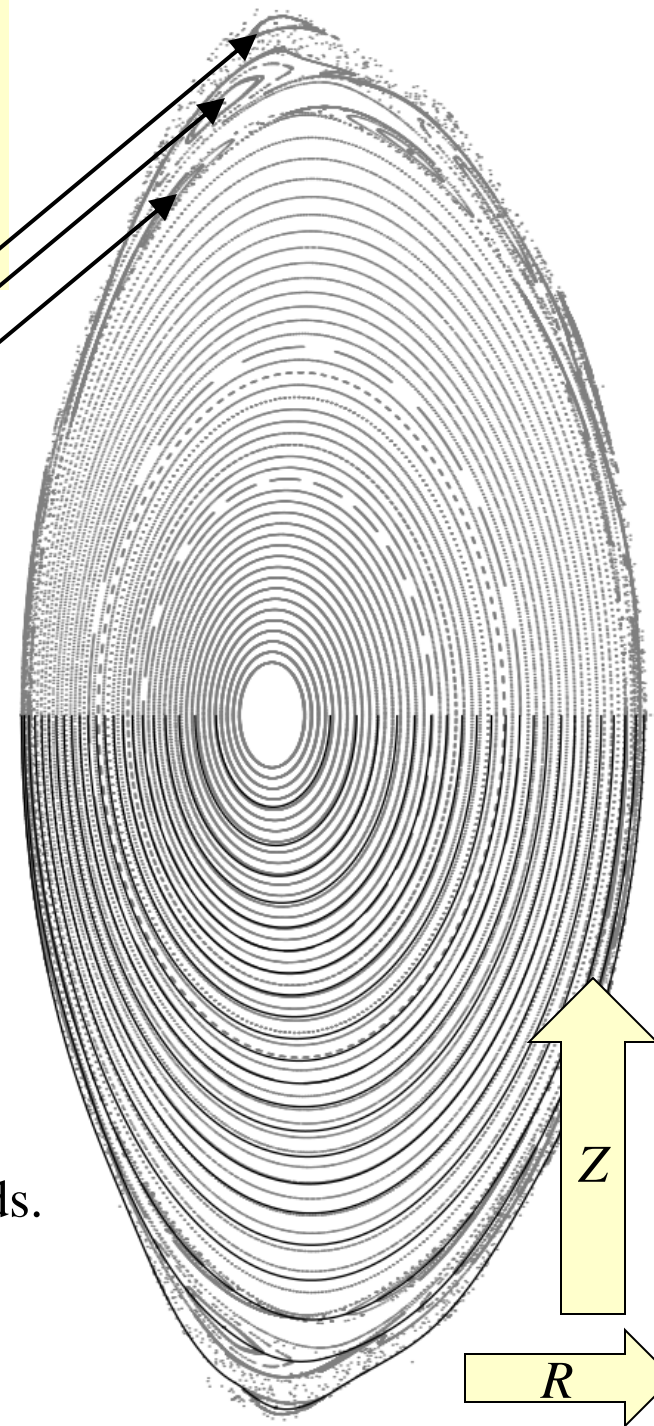
$(10,5)$   
 $(10,6)$   
 $(10,7)$

The magnetic field is provided by HINT2,  
(but this calculation is for the standard vacuum configuration.)

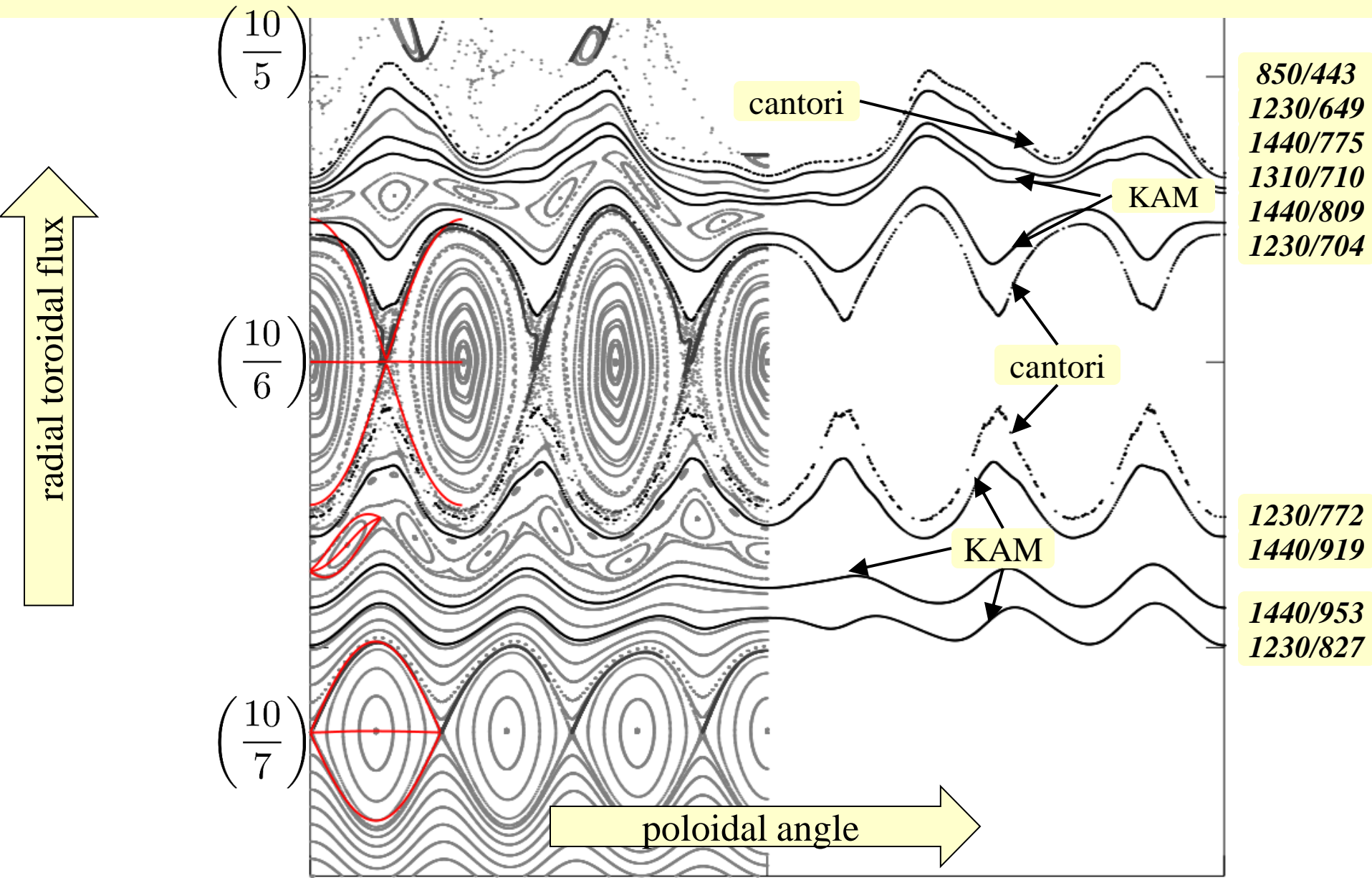
A selection of QFM surfaces is constructed,  
shown with black lines, with periodicities:

$(10,23), (10,22), (10,21), \dots$  (near axis)  
 $\dots, (10,9), (10,8), (10,7), (10,6)$ , (near edge)

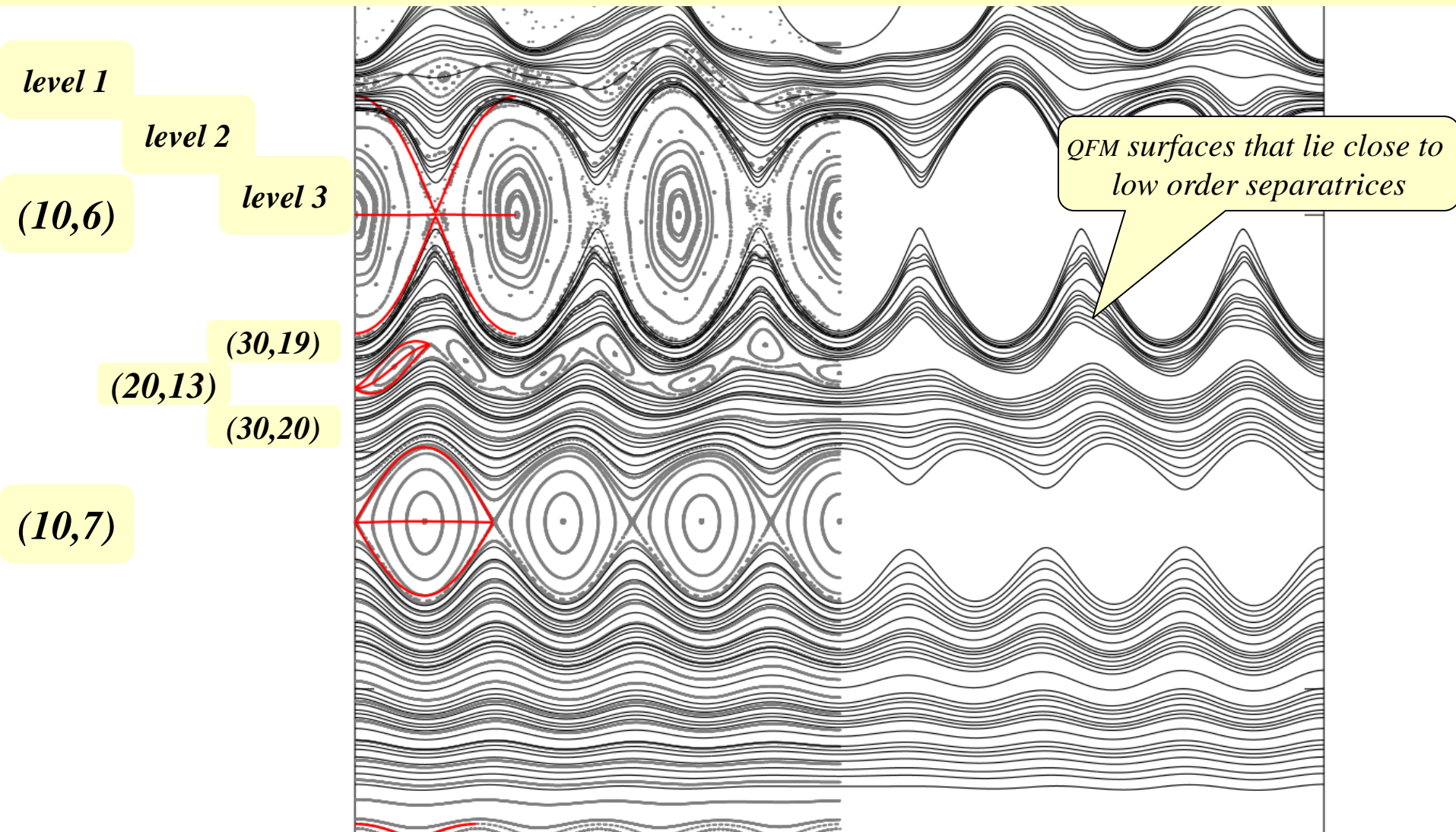
Following slides will concentrate on edge region  
between the  $(10,9), (10,8), (10,7), (10,6)$  and  $(10,5)$  islands.



Near the edge, there is a fractal mix of low-order islands, high-order islands, KAM surfaces, cantori, etc



Now, back to the edge of LHD:  
construct a set of high-order QFM surfaces, . . .

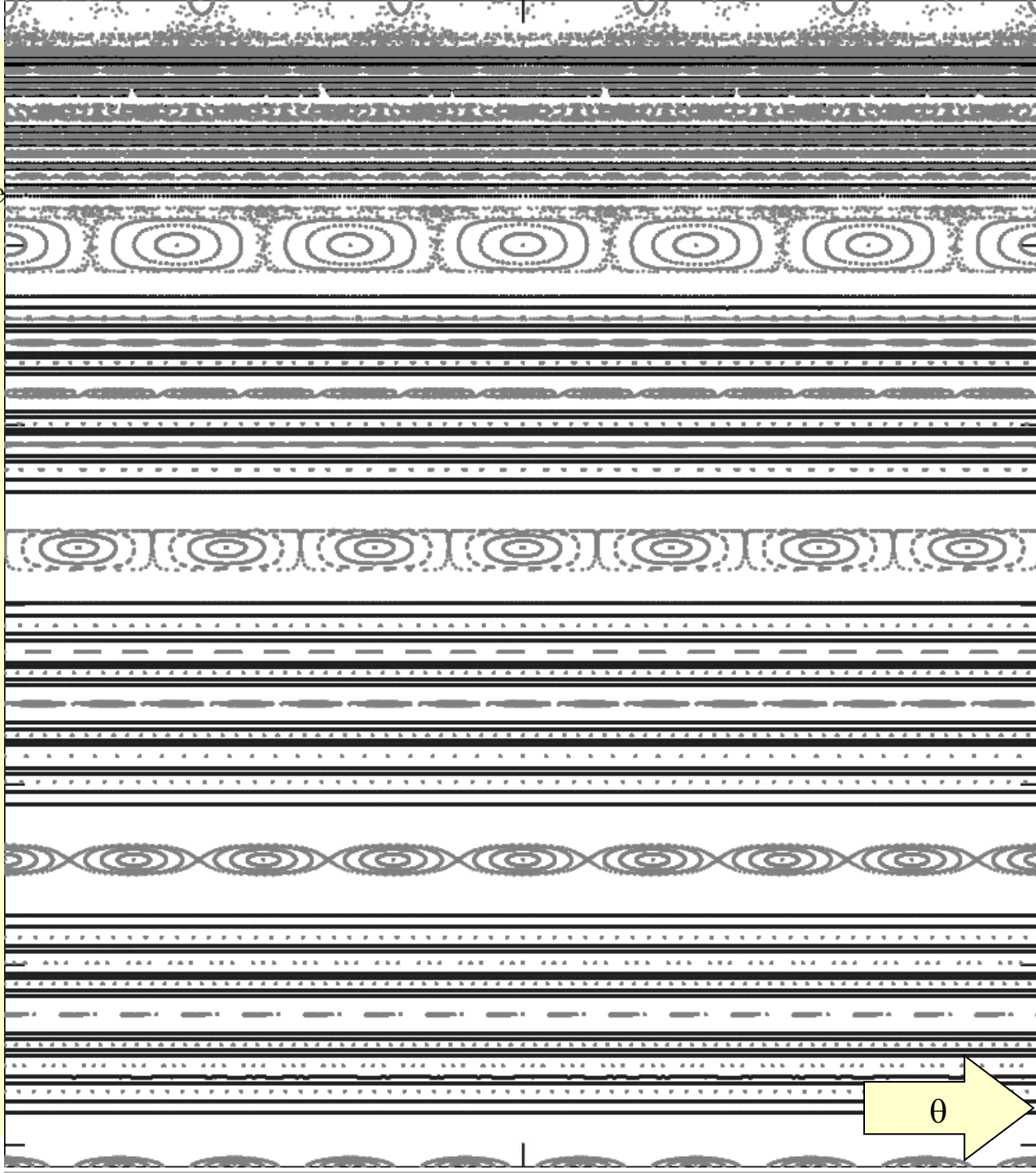
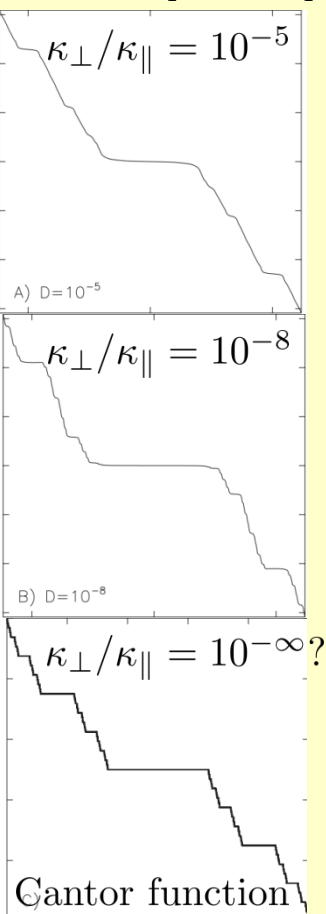


and use these surfaces as coordinate surfaces . . .

# Poincaré plot.

Assuming no source in islands,  
 $T \approx T(\rho)$ ,  
 $p \approx p(\rho)$ .

Numerical Solution  
to anisotropic transport



$$\left(\frac{10}{5}\right)$$

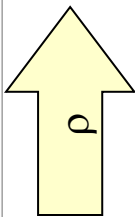
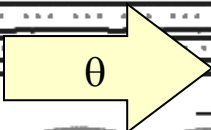
$$\left(\frac{20}{11}\right)$$

$$\left(\frac{10}{6}\right)$$

$$\left(\frac{10}{7}\right)$$

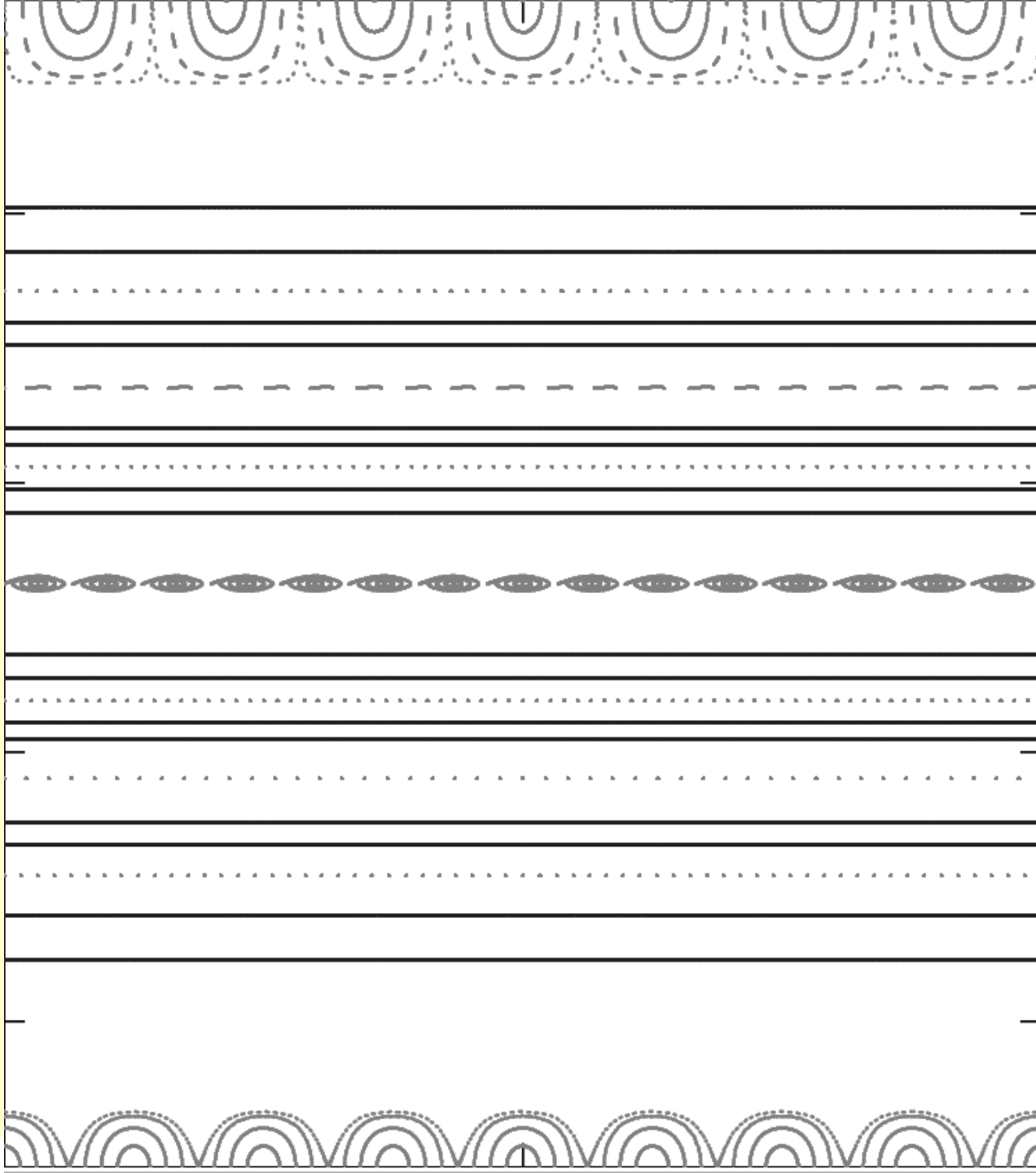
$$\left(\frac{10}{8}\right)$$

$$\left(\frac{10}{9}\right)$$





Poincaré  
plot.



$$\left(\frac{10}{7}\right)$$

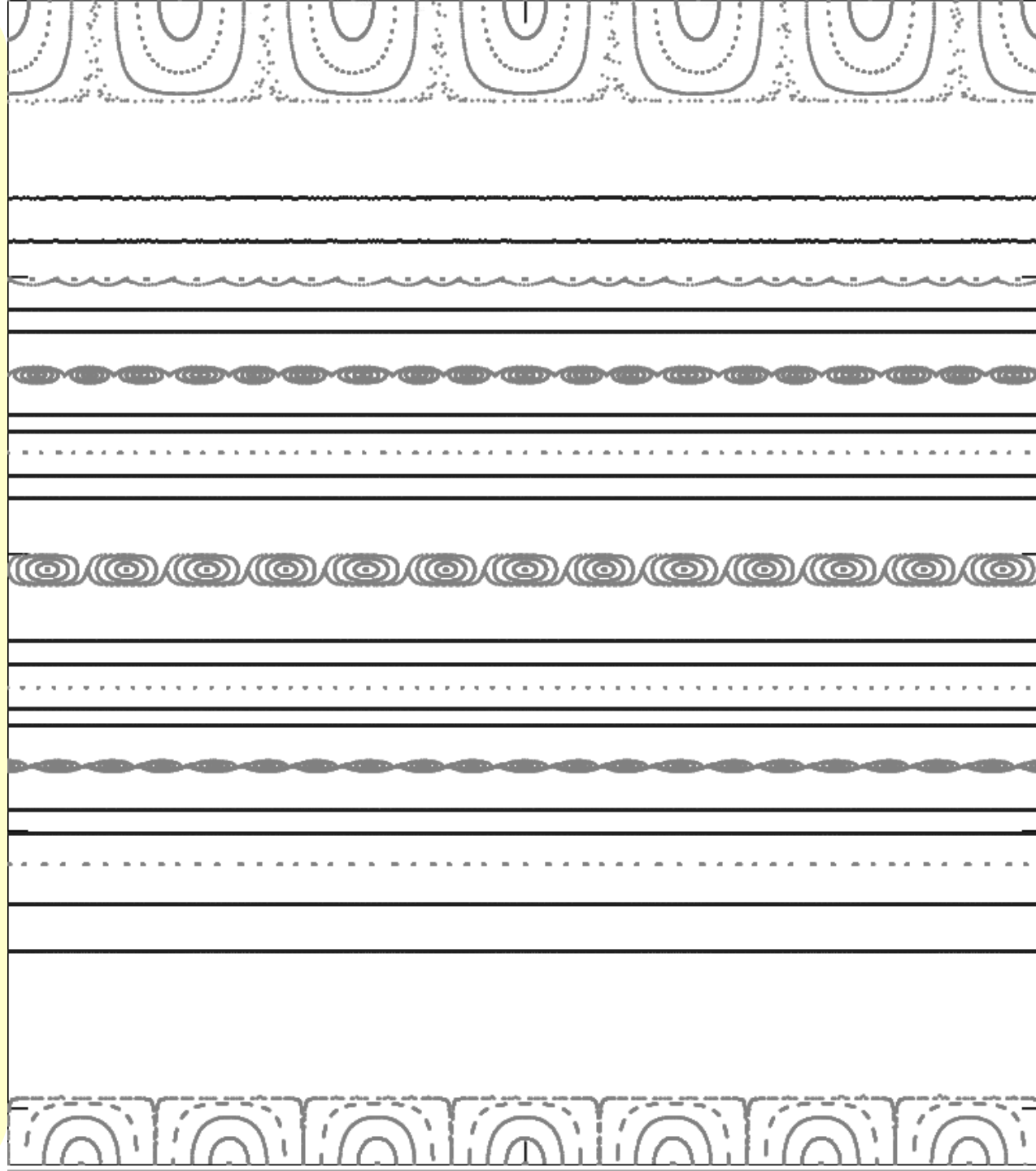
$$\left(\frac{30}{22}\right)$$

$$\left(\frac{20}{15}\right)$$

$$\left(\frac{30}{23}\right)$$

$$\left(\frac{10}{8}\right)$$

Poincaré  
plot.



$$\left(\frac{10}{6}\right)$$

$$\left(\frac{30}{19}\right)$$

$$\left(\frac{20}{13}\right)$$

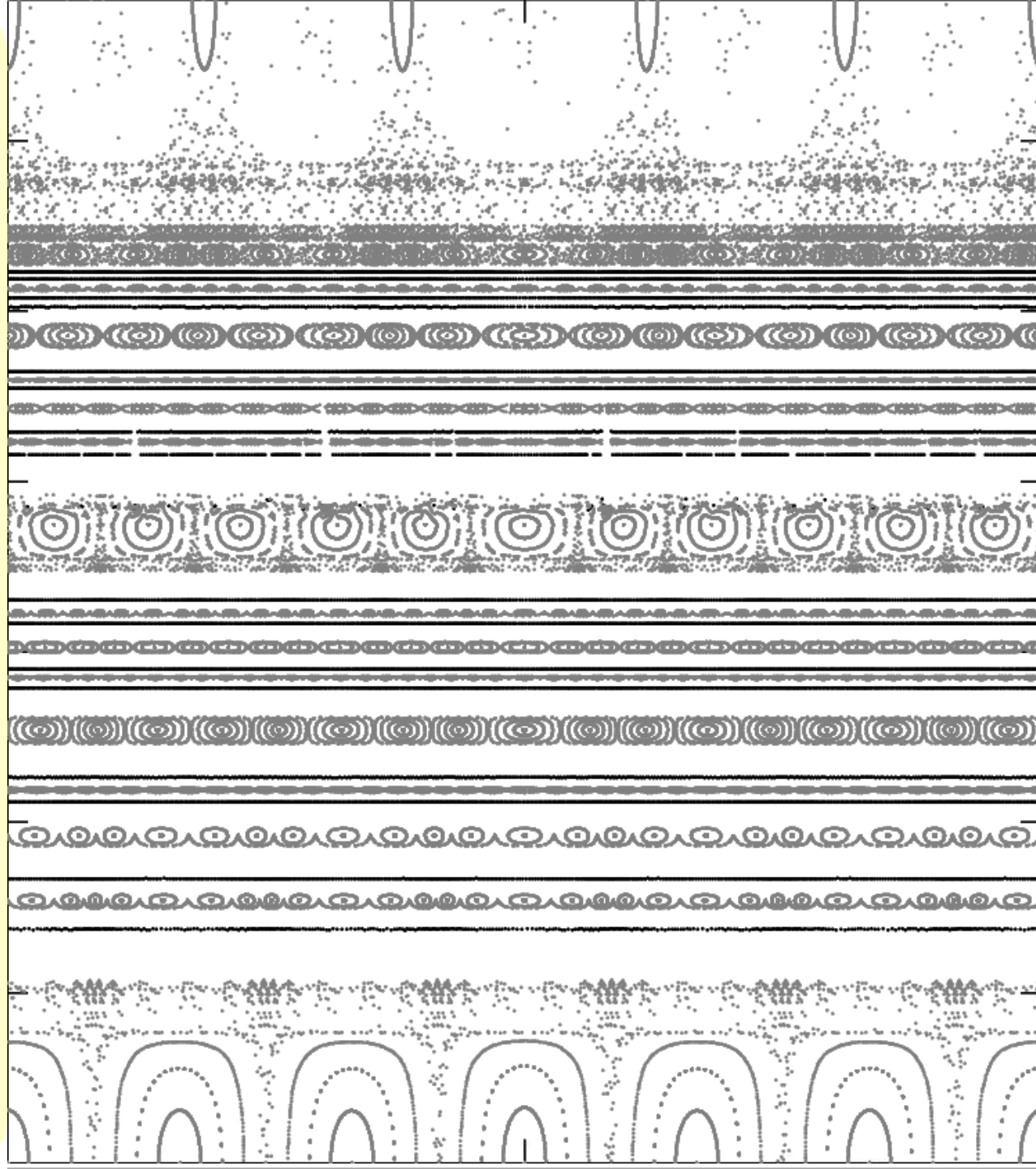
$$\left(\frac{30}{20}\right)$$

Islands become  
square.

$$\left(\frac{10}{7}\right)$$



Poincaré  
plot.



$\begin{pmatrix} 40 \\ 21 \end{pmatrix}$

$\begin{pmatrix} 30 \\ 16 \end{pmatrix}$

$\begin{pmatrix} 30 \\ 27 \end{pmatrix}$

$\begin{pmatrix} 20 \\ 11 \end{pmatrix}$

$\begin{pmatrix} 30 \\ 28 \end{pmatrix}$

$\begin{pmatrix} 30 \\ 17 \end{pmatrix}$

$\begin{pmatrix} 40 \\ 23 \end{pmatrix}$

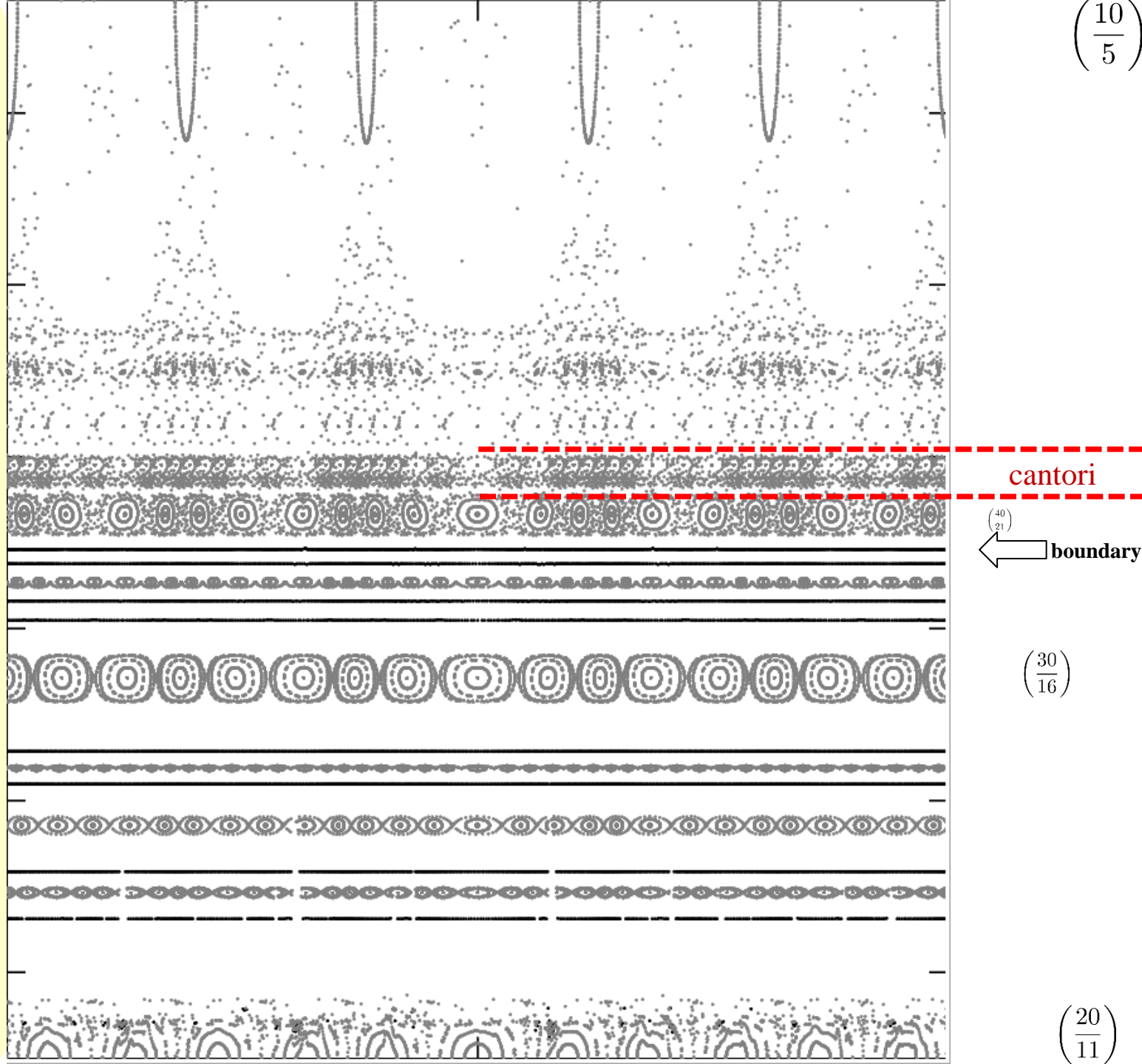
$\begin{pmatrix} 10 \\ 6 \end{pmatrix}$

# Poincaré plot.

Edge of confinement region is not a single, sharp barrier;

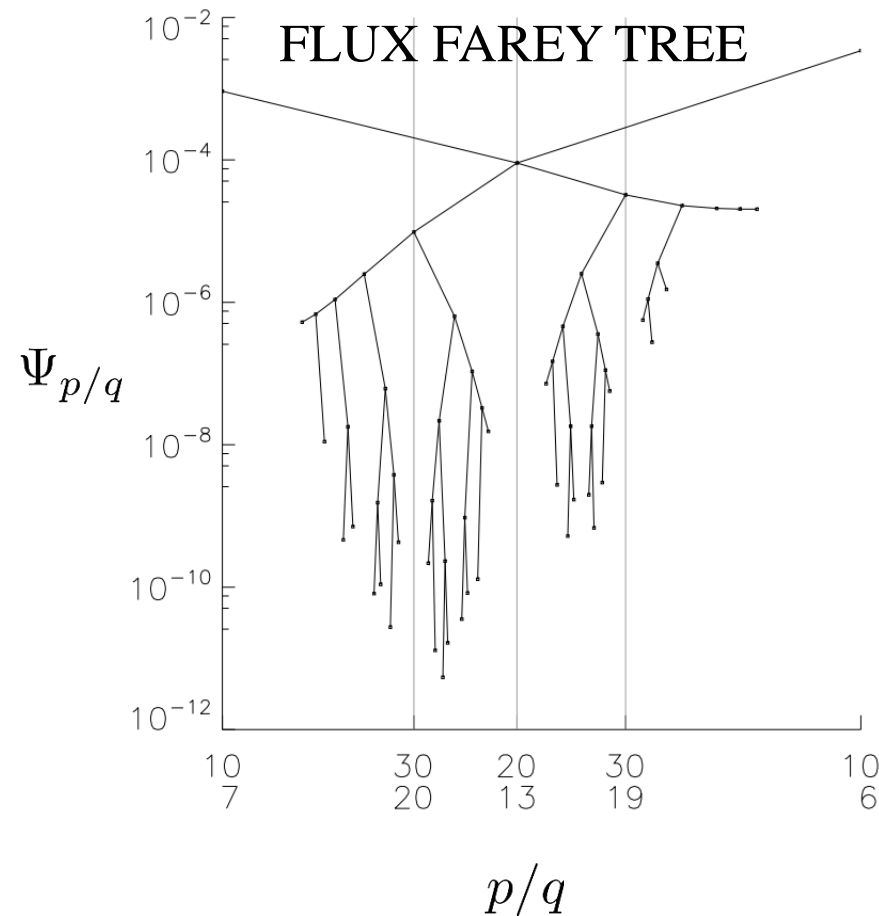
but instead a hierarchy of

- i. islands,
- ii. KAM, and
- iii. Cantori.



The Flux Farey-tree shows the flux across the rational surfaces; the importance of each of the hierarchy of partial barriers can be quantified.

$$\Psi_{p/q} \equiv \int_O \mathbf{A} \cdot d\mathbf{l} - \int_X \mathbf{A} \cdot d\mathbf{l}$$



# Ongoing research efforts:

## Possible collaborations:

- incorporate chaotic-coordinates into HINT2, M3D-C<sub>1</sub>, NIMROD, ... as post-processor diagnostic;
- revise coordinate interpolation between QFM surfaces, so that interpolated surfaces do not intersect;
- revise coordinate extrapolation past outermost QFM surface into the separatrix that surrounds the plasma, and beyond . . .
- re-visit comparison between ghosts & QFM surfaces ;
- re-visit how useful chaotic coordinates are for solving the anisotropic diffusion equation;

# Relevant publications:

<http://w3.pppl.gov/~shudson/bibliography.html>

**Chaotic coordinates for the Large Helical Device**, S.R.Hudson & Y. Suzuki

Physics of Plasmas, 21:11xxxx, 2014.

**Generalized action-angle coordinates defined on island chains**, R.L.Dewar, S.R.Hudson & A.M.Gibson

Plasma Physics and Controlled Fusion, 55:014004, 2013

**Unified theory of Ghost and Quadratic-Flux-Minimizing Surfaces**, R. L.Dewar, S. R.Hudson & A. M.Gibson

Journal of Plasma and Fusion Research SERIES, 9:487, 2010

**Are ghost surfaces quadratic-flux-minimizing?**, S.R.Hudson & R.L.Dewar

Physics Letters A, 373(48):4409, 2009

**An expression for the temperature gradient in chaotic fields**, S.R.Hudson

Physics of Plasmas, 16:010701, 2009

**Temperature contours and ghost-surfaces for chaotic magnetic fields**, S.R.Hudson & J.Breslau

Physical Review Letters, 100:095001, 2008

**Calculation of cantori for Hamiltonian flows**, S.R.Hudson

Physical Review E, 74:056203, 2006

**Almost invariant manifolds for divergence free fields**, R.L.Dewar, S.R.Hudson & P.Price

Physics Letters A, 194(1-2):49, 1994



# To illustrate, we examine the standard configuration of LHD

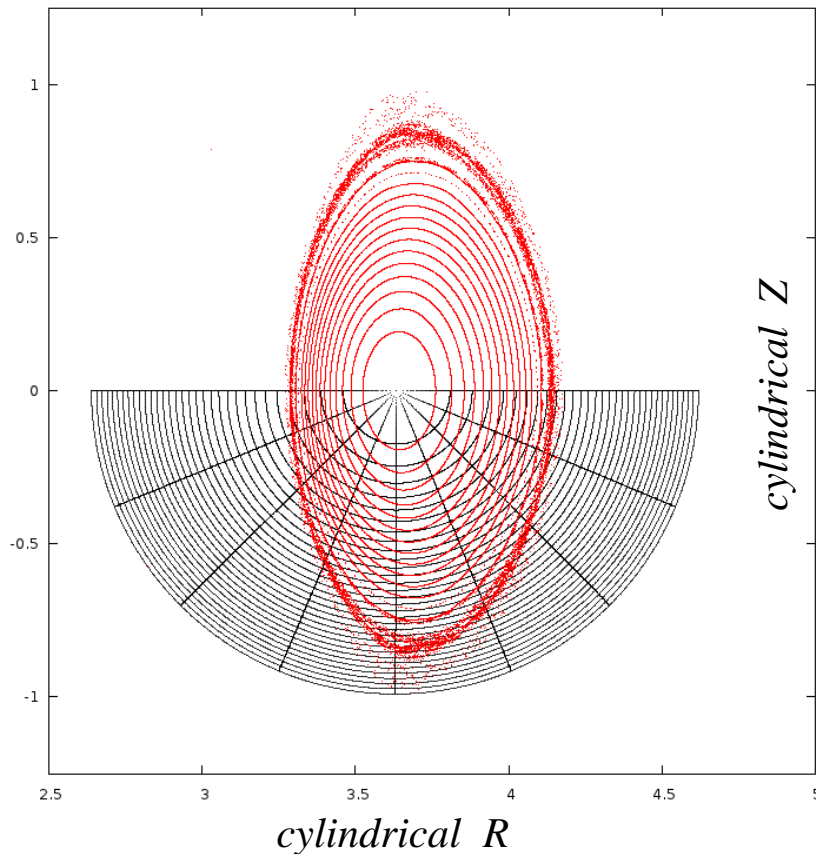
The initial coordinates are axisymmetric, circular cross section,

$$R = 3.63 + \rho \cdot 0.9 \cos\vartheta$$

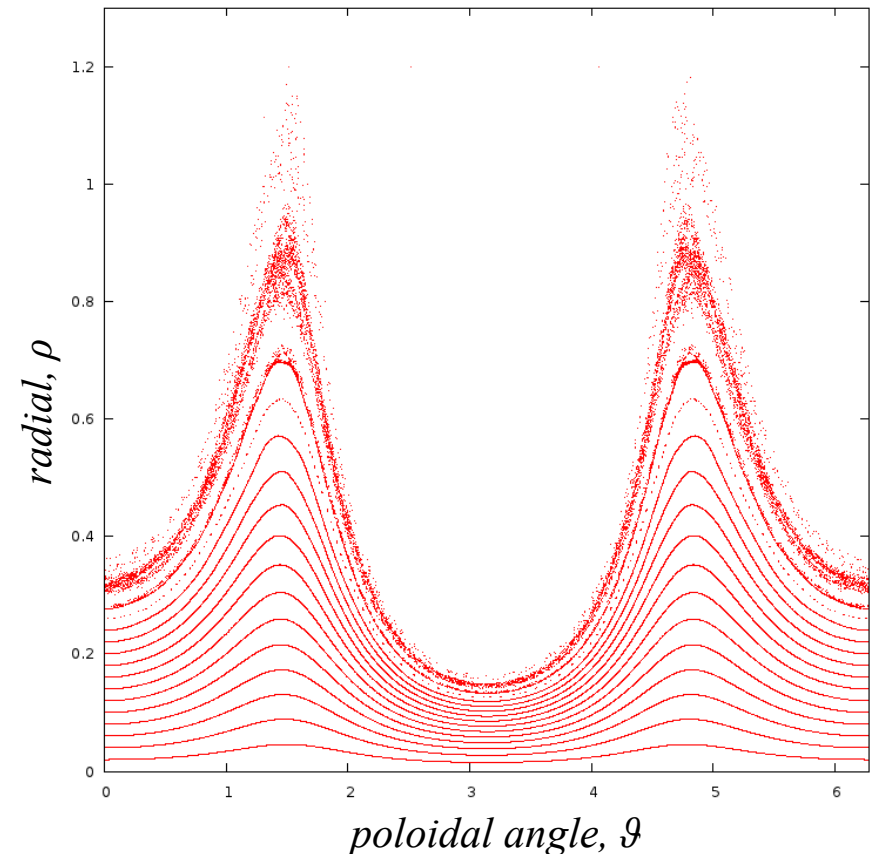
$$Z = \rho \cdot 0.9 \sin\vartheta$$

which are *not* a good approximation to flux coordinates!

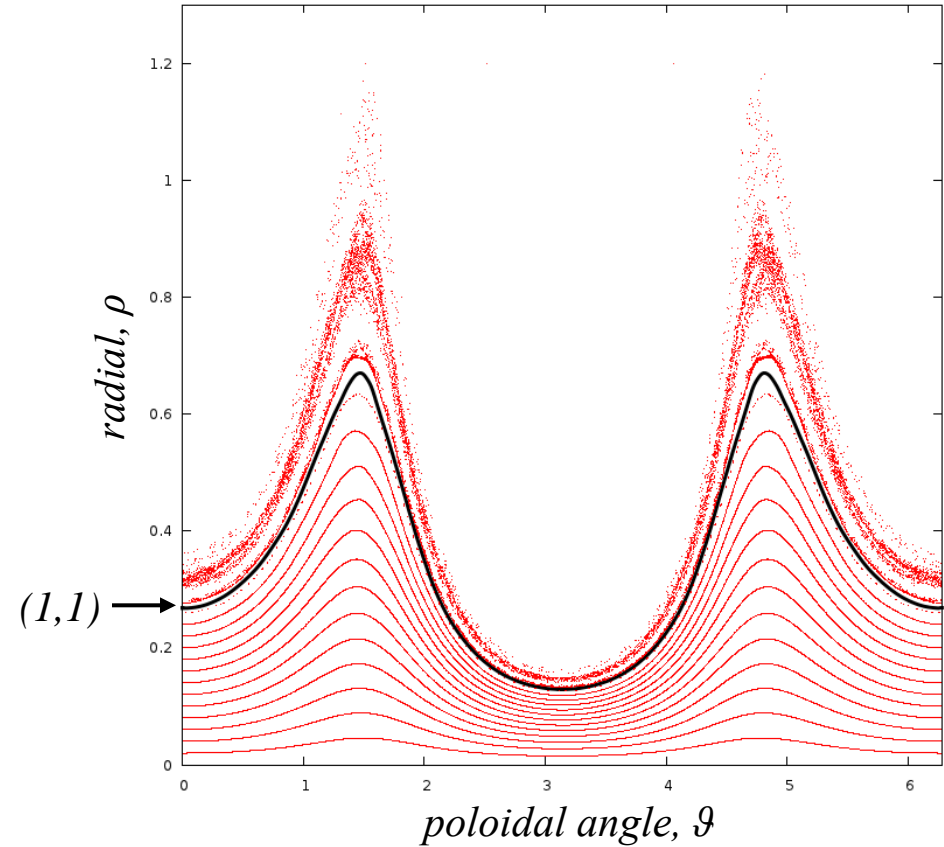
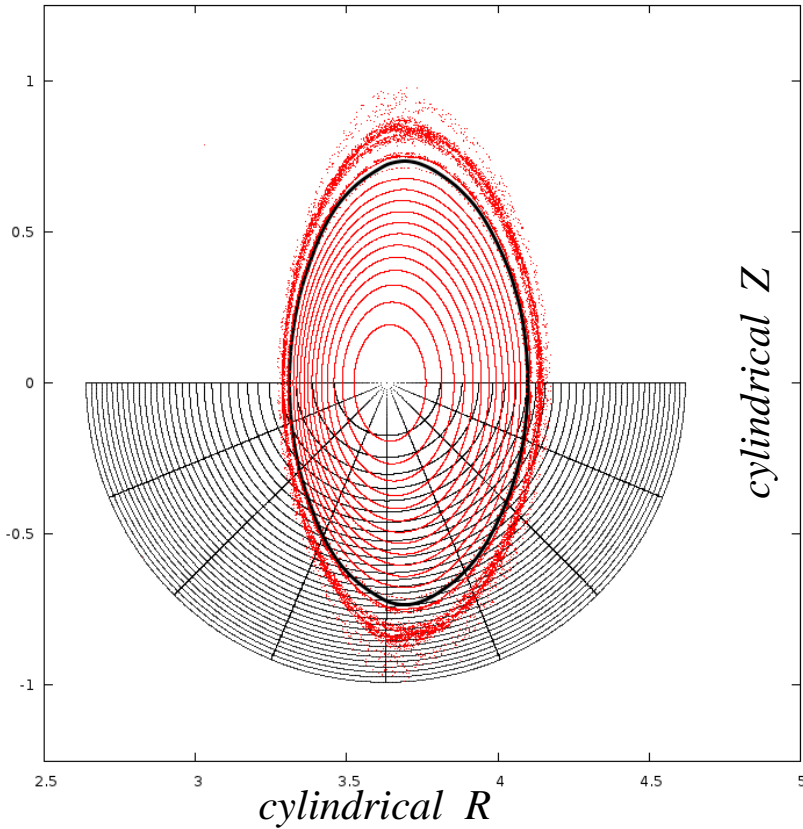
**Poincaré plot in cylindrical coordinates**



**Poincaré plot in toroidal coordinates**



We construct coordinates that *better* approximate straight-field line flux coordinates, by constructing a set of rational, almost-invariant surfaces, e.g. the (1,1), (1,2) surfaces



838 / 841

A Fourier representation of the (1,1) rational surface is constructed,

$$R = R(\alpha, \zeta) = \sum R_{m,n} \cos(m \alpha - n \zeta)$$

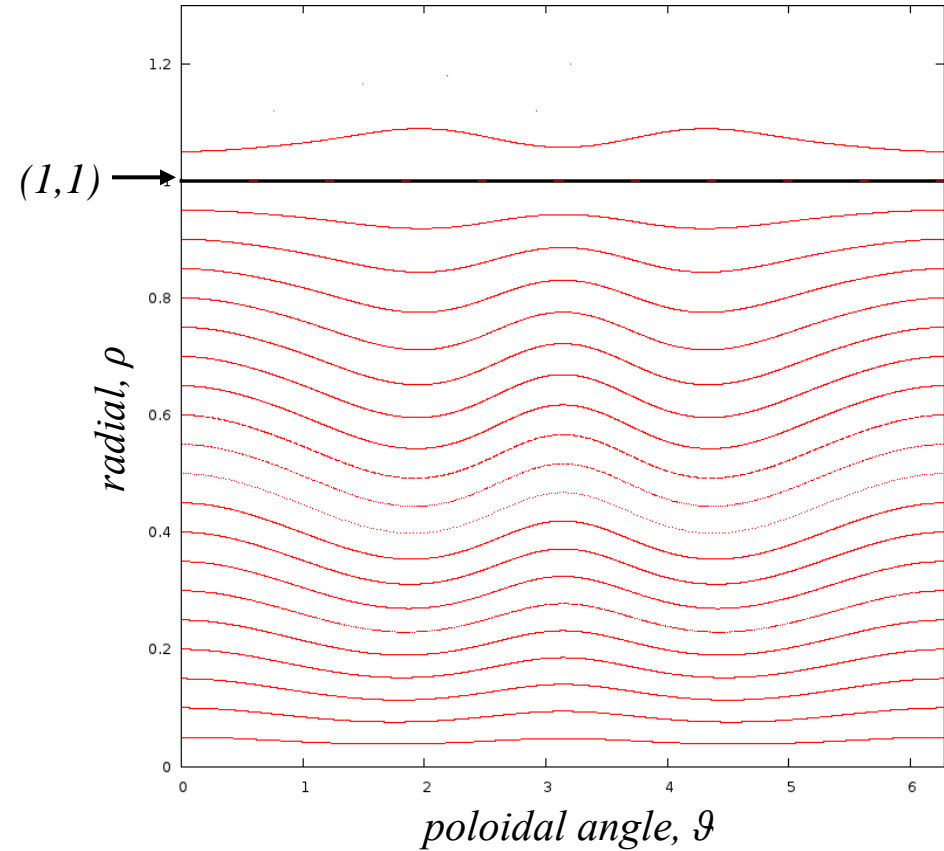
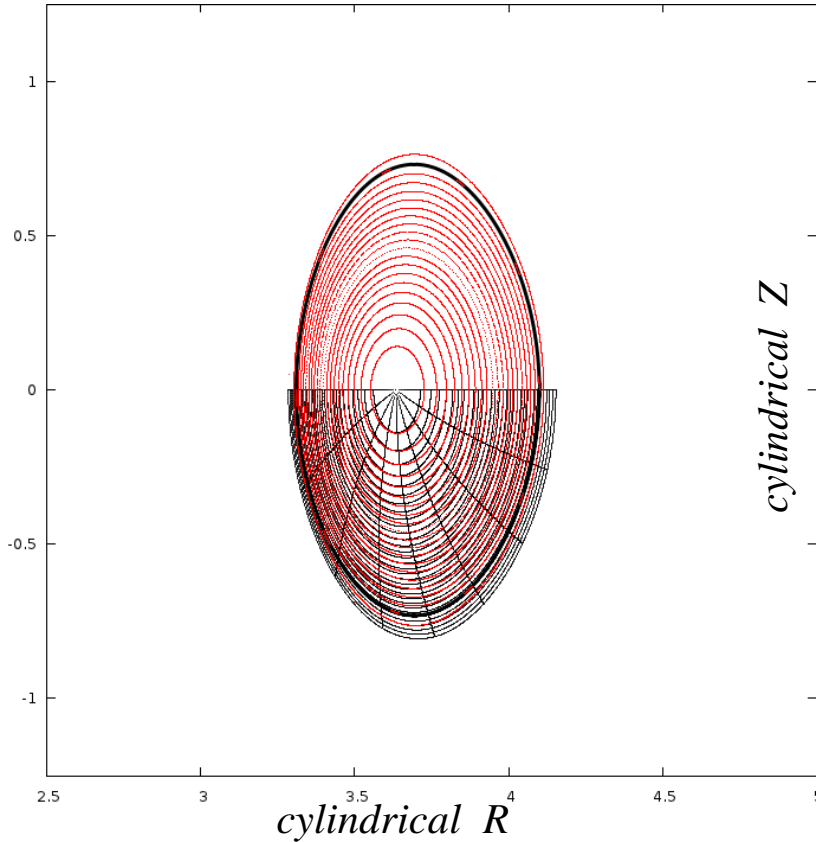
$$Z = Z(\alpha, \zeta) = \sum Z_{m,n} \sin(m \alpha - n \zeta),$$

where  $\alpha$  is a straight field line angle

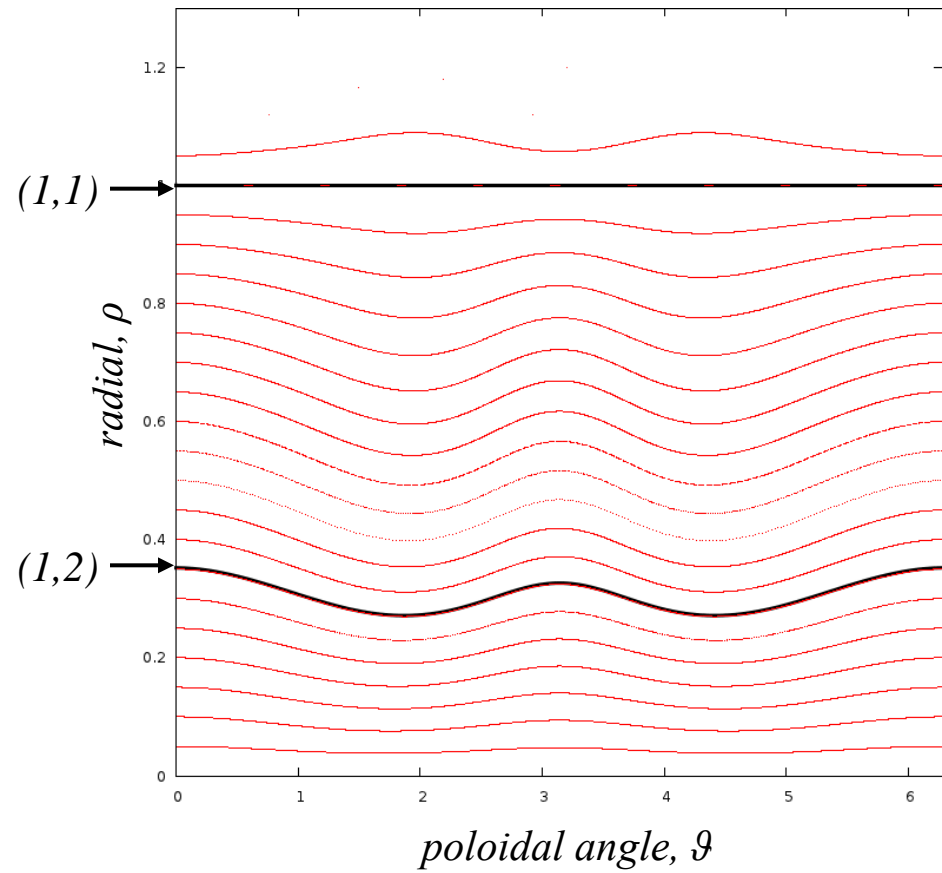
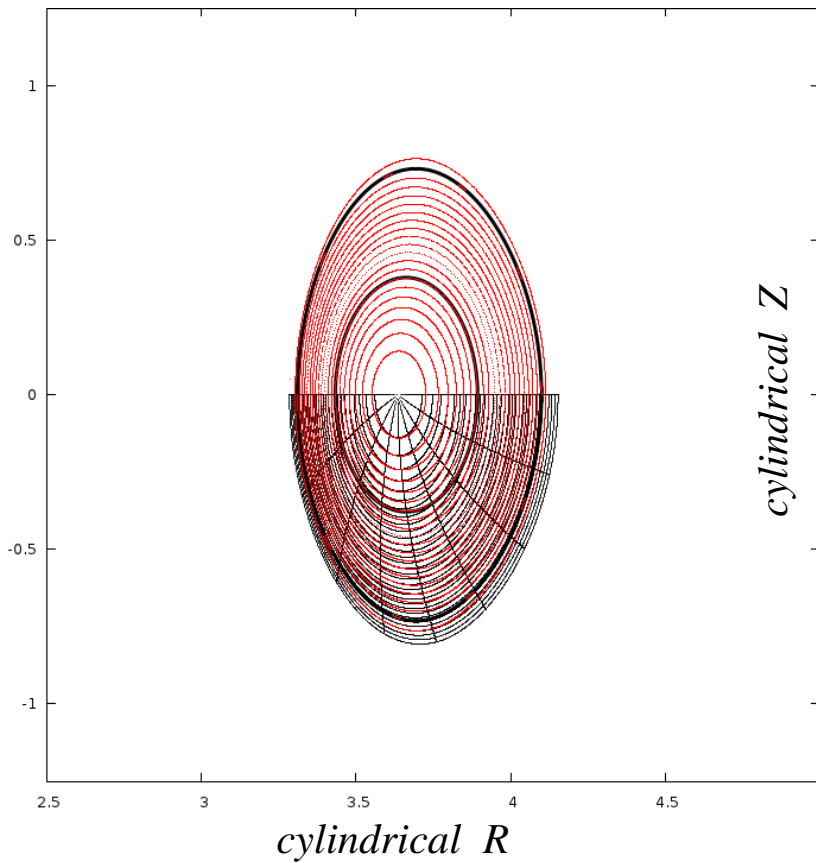


Updated coordinates:  
the (1,1) surface is used as a coordinate surface.

The updated coordinates are a better approximation to straight-field line flux coordinates, and the flux surfaces are (almost) flat



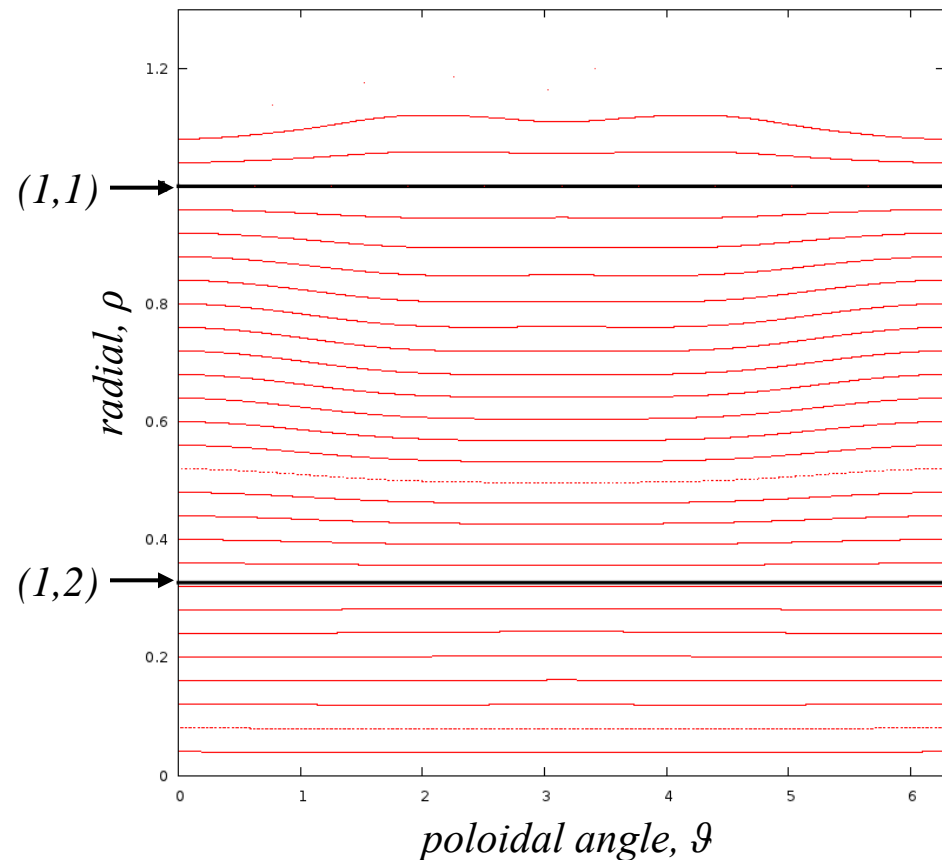
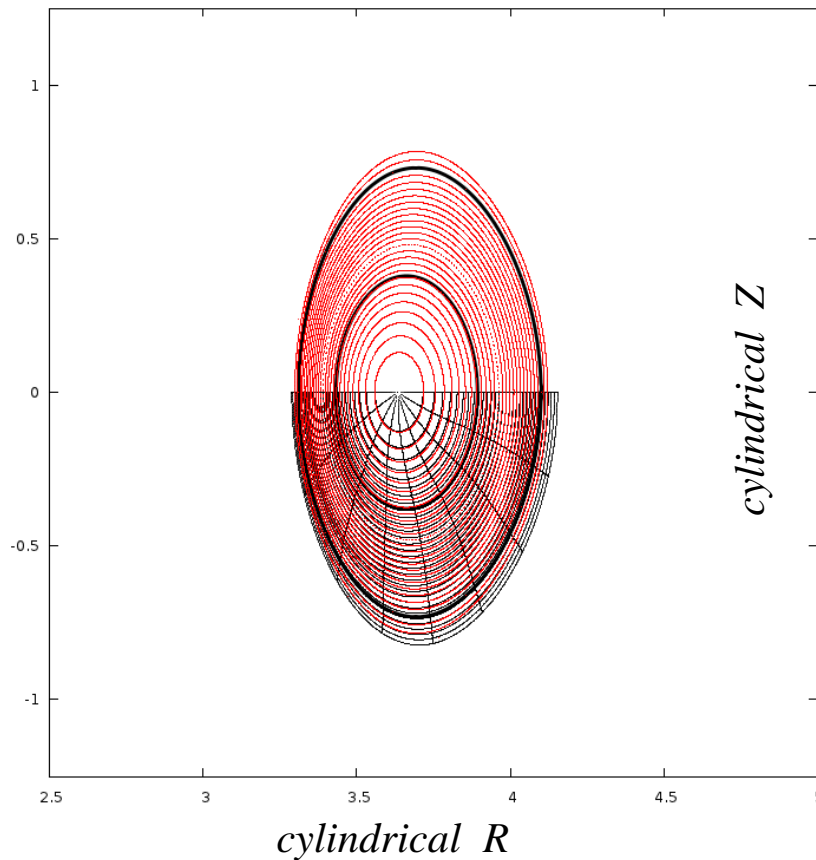
# Now include the (1,2) rational surface



Updated coordinates:

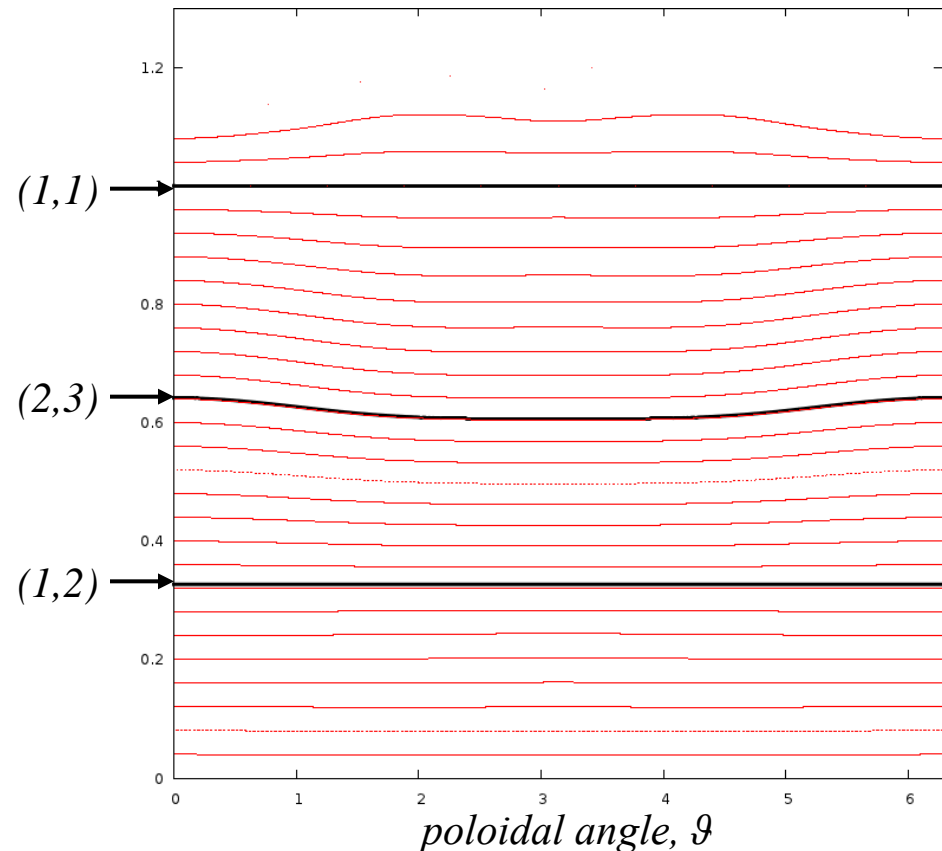
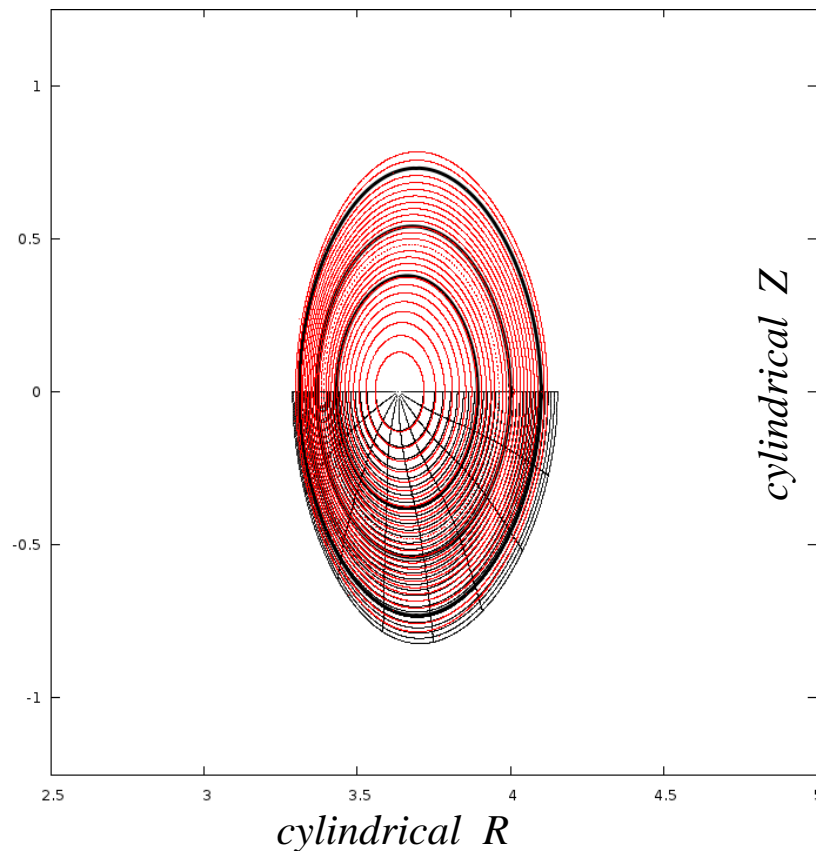
the (1,1) surface is used as a coordinate surface

the (1,2) surface is used as a coordinate surface



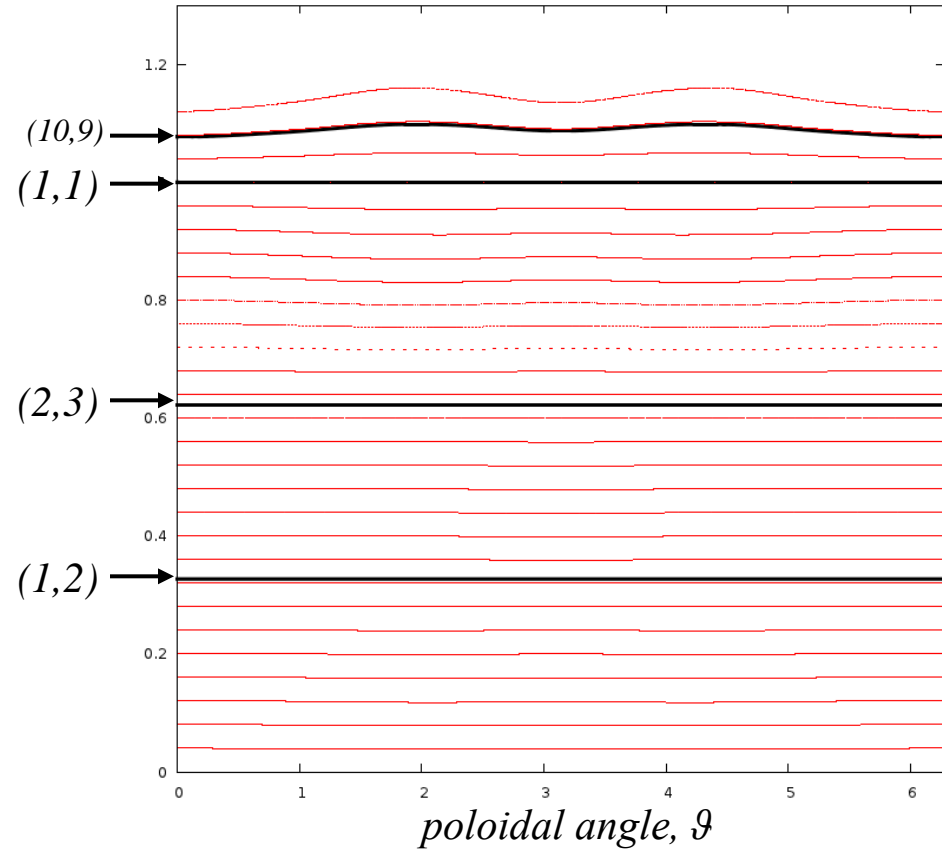
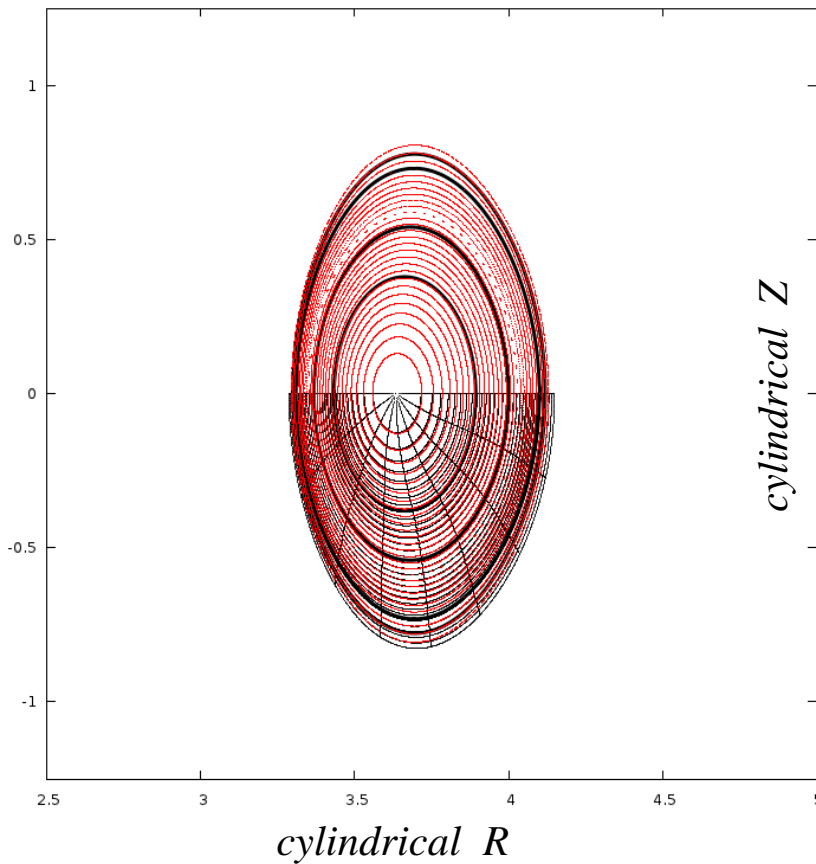
# Now include the (2,3) rational surface

Note that the (1,1) and (1,2) surfaces have previously been constructed and are used as coordinate surfaces, and so these surfaces are flat.



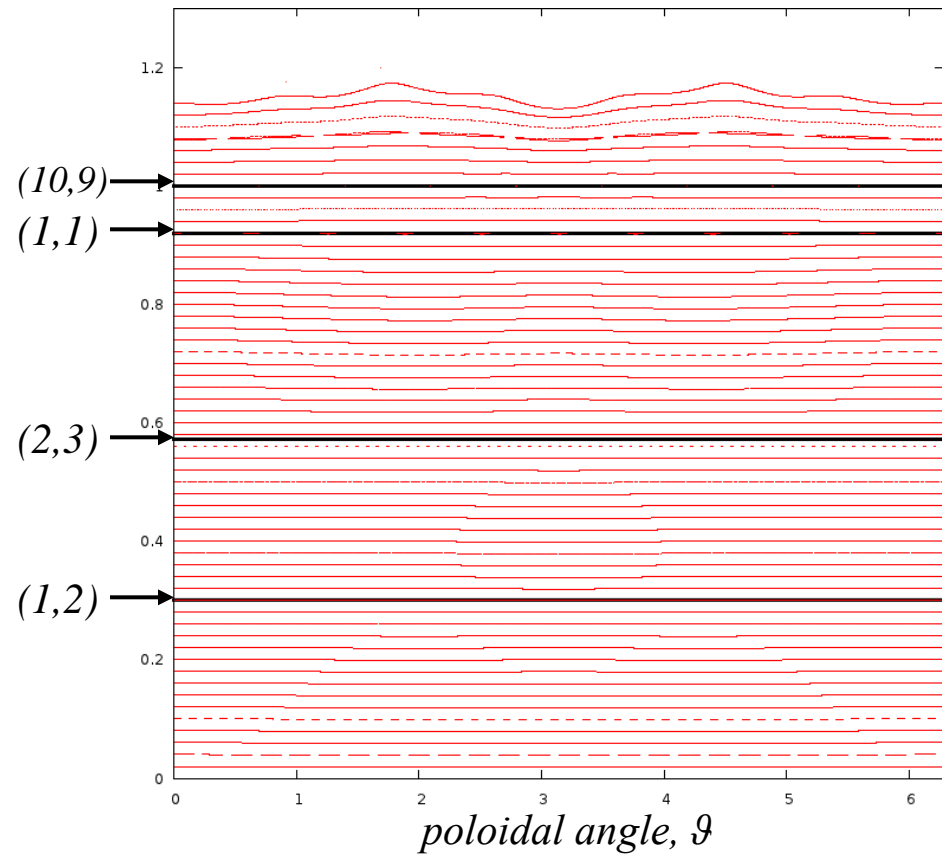
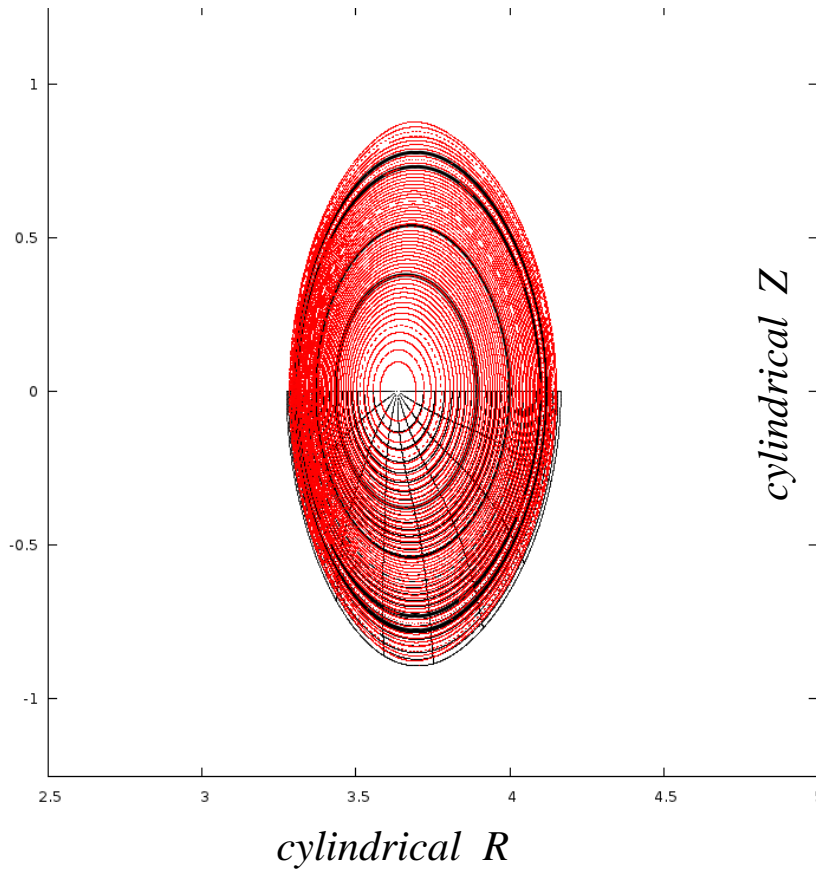
# Updated Coordinates:

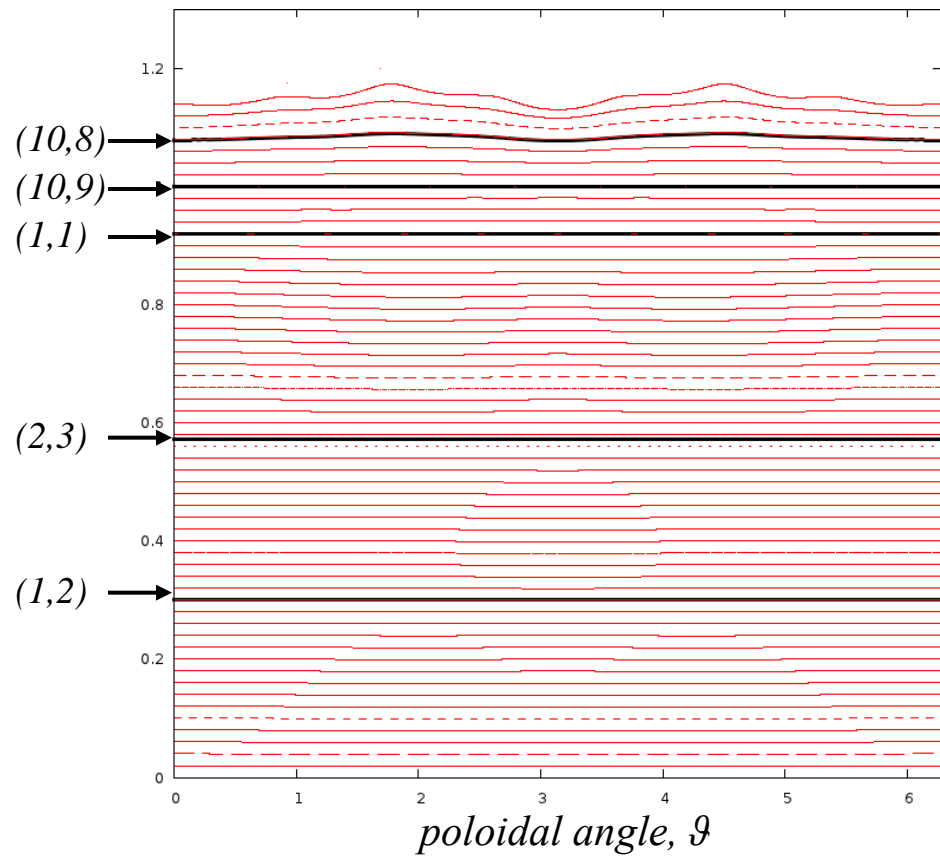
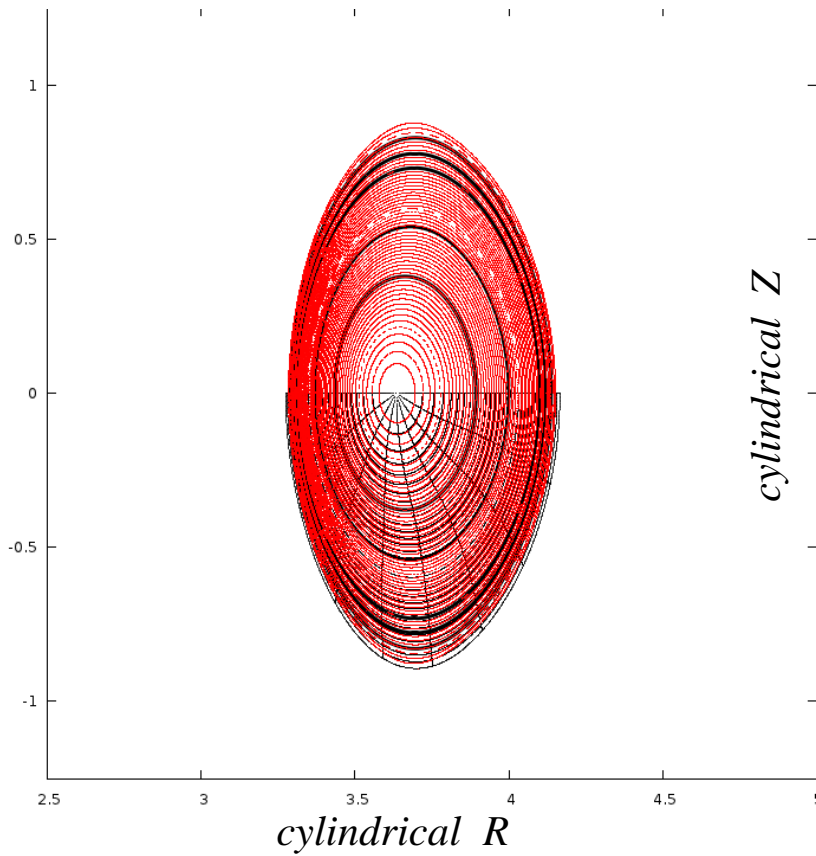
the (1,1), (2,3) & (1,2) surfaces are used as coordinate surfaces

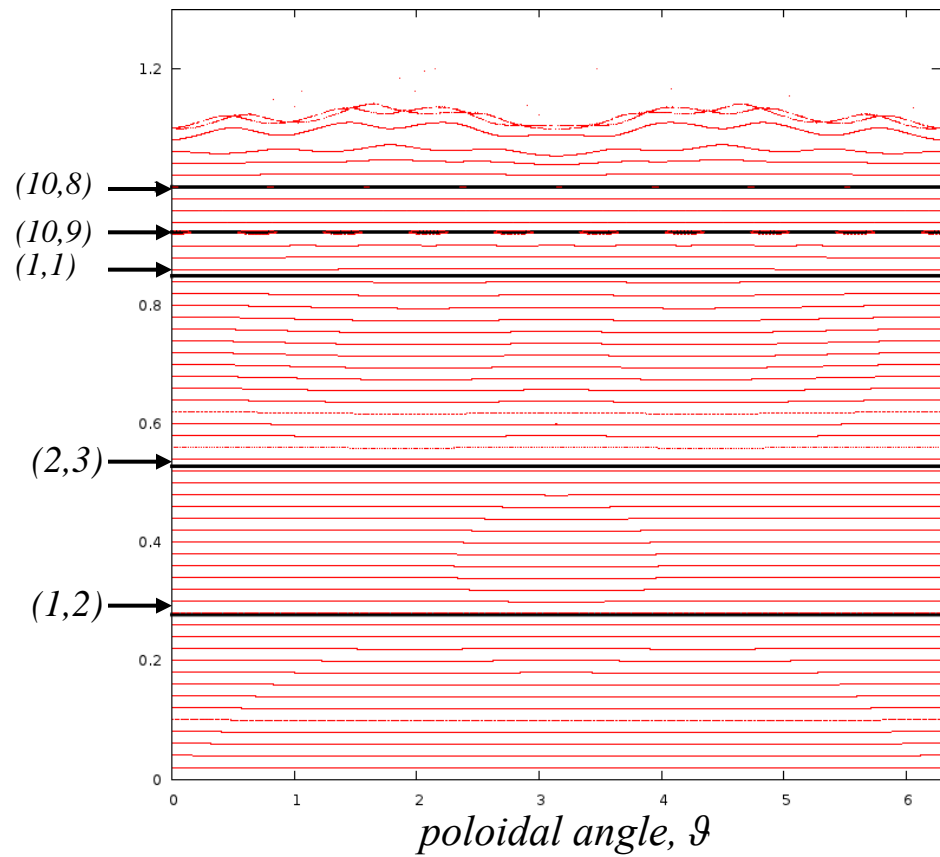
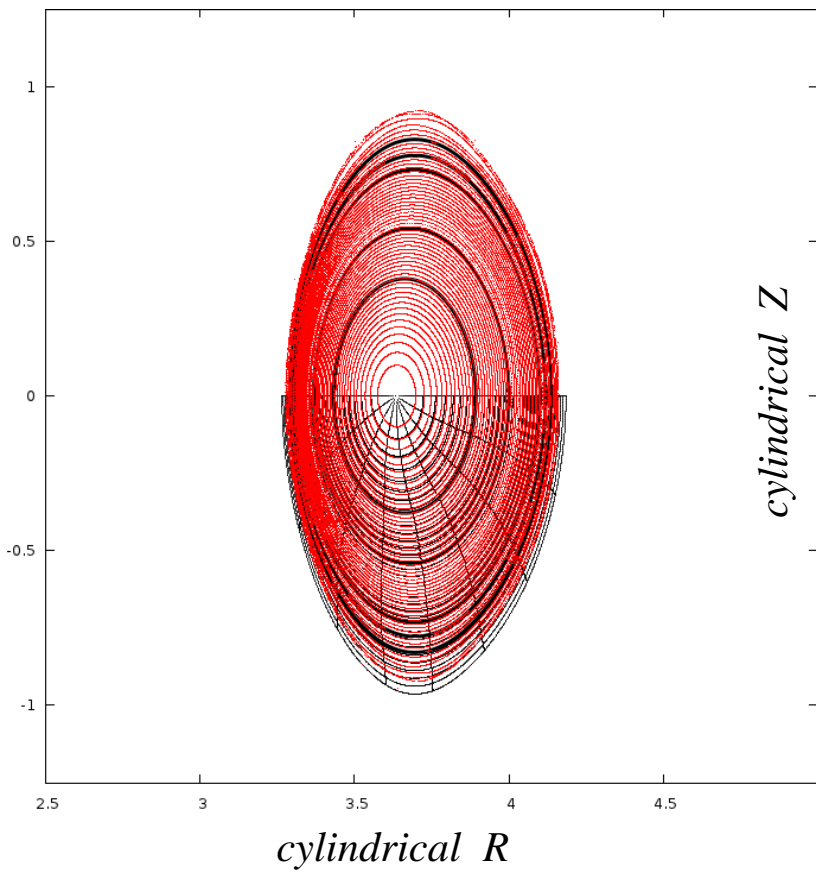


New Coordinates, the (10,9) surface is used as the coordinate boundary  
 the (1,1) surface is used as a coordinate surface  
 the (2,3) surface is used as a coordinate surface  
 the (1,2) surface is used as a coordinate surface

*Poincare plot*

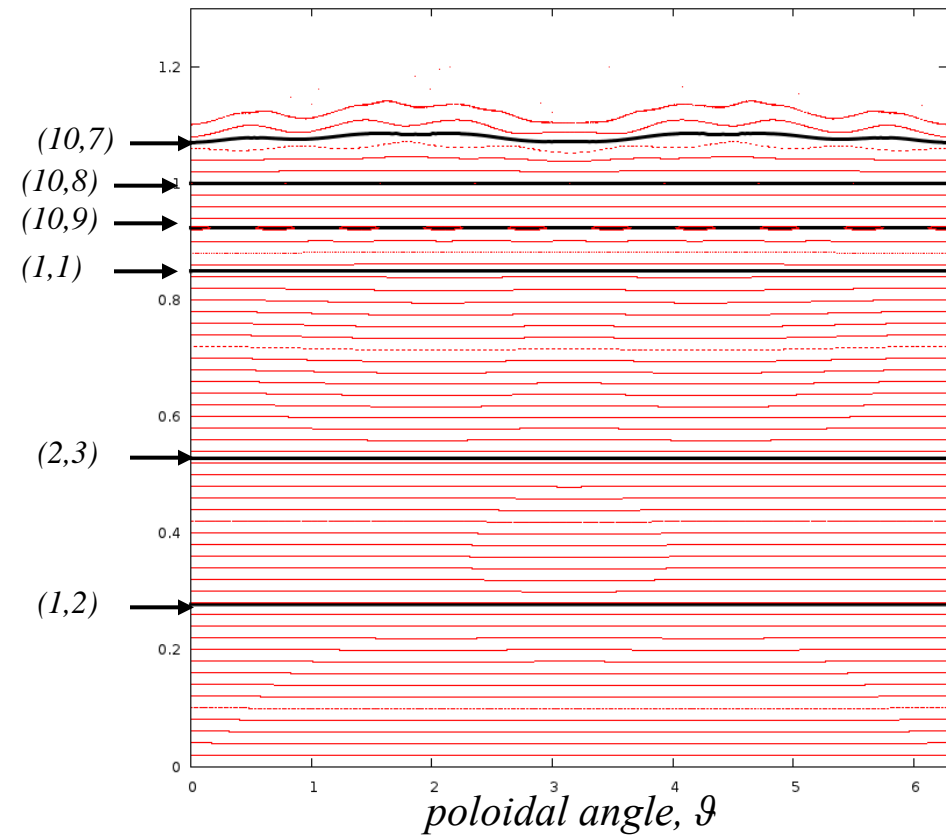
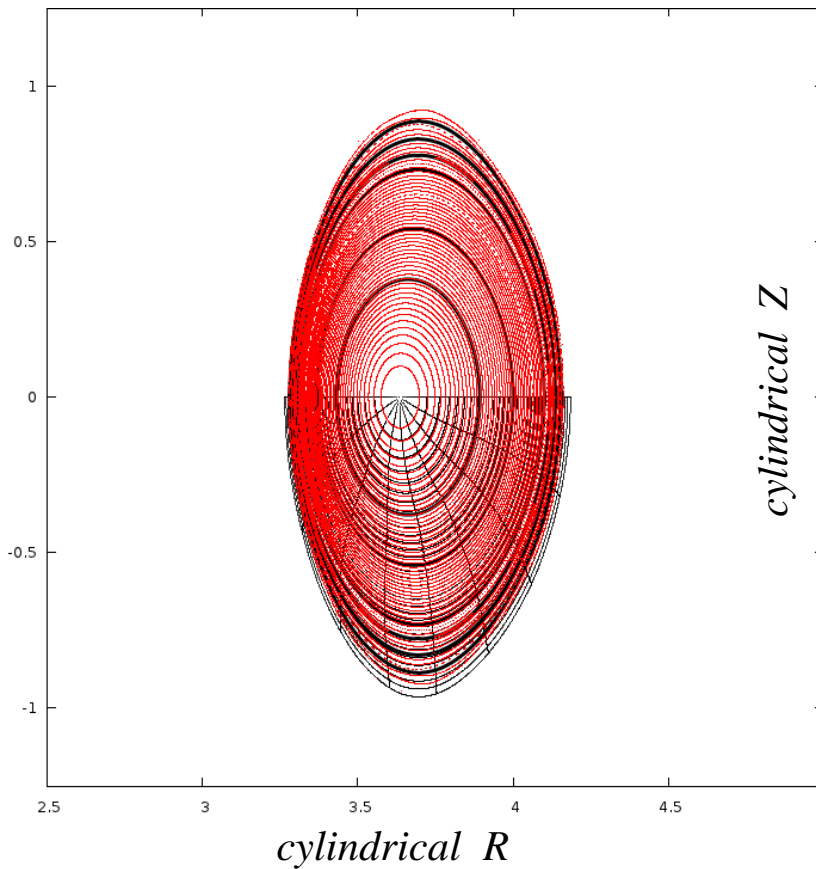




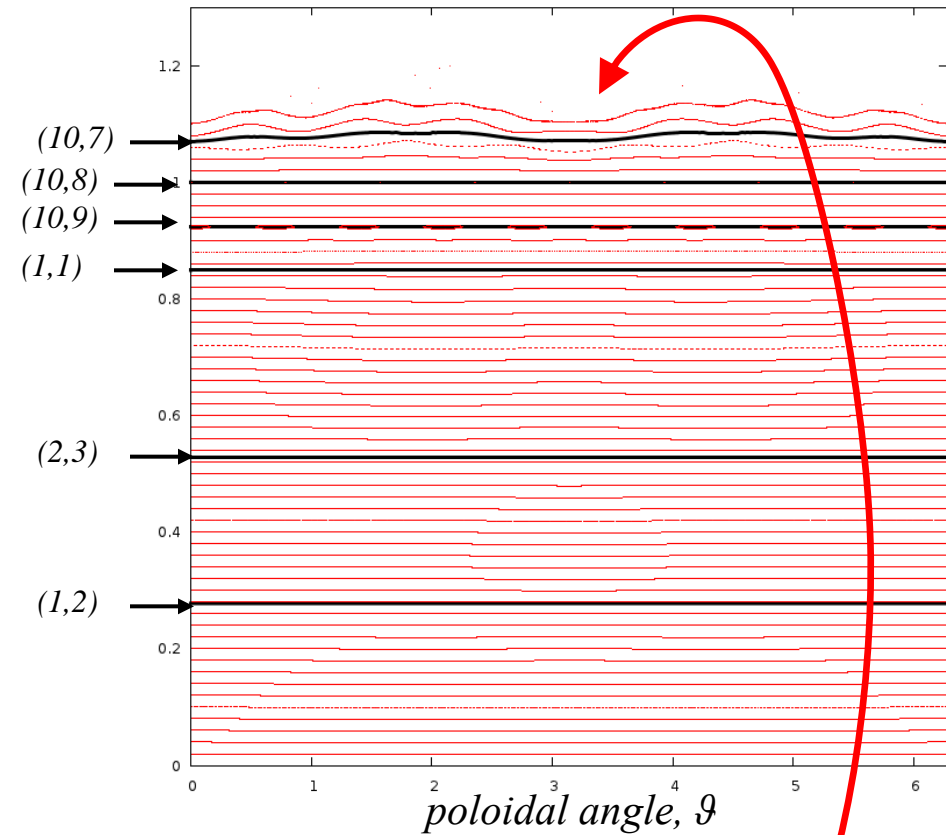
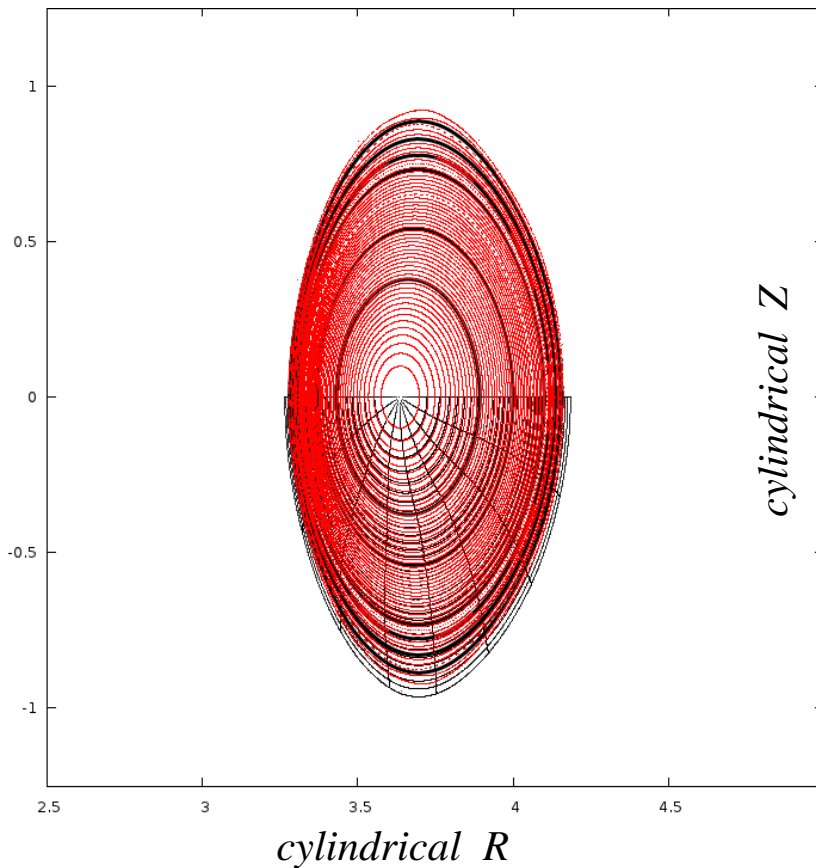




Straight field line coordinates can be constructed over the domain where invariant flux surfaces exist

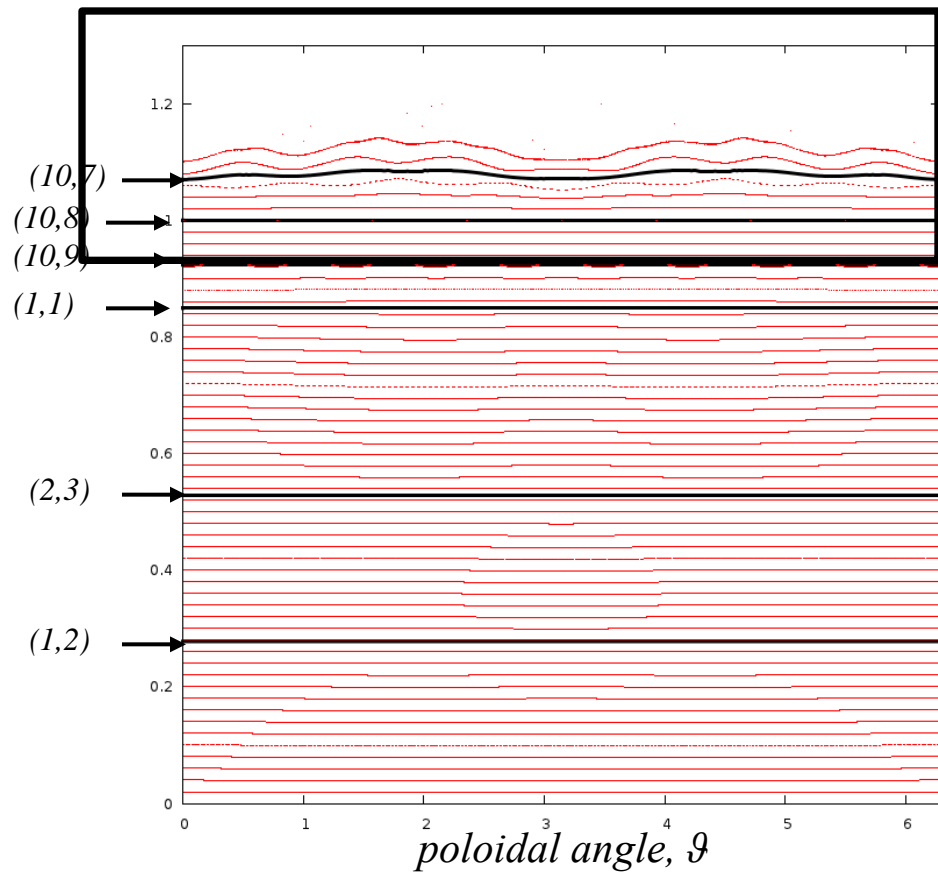
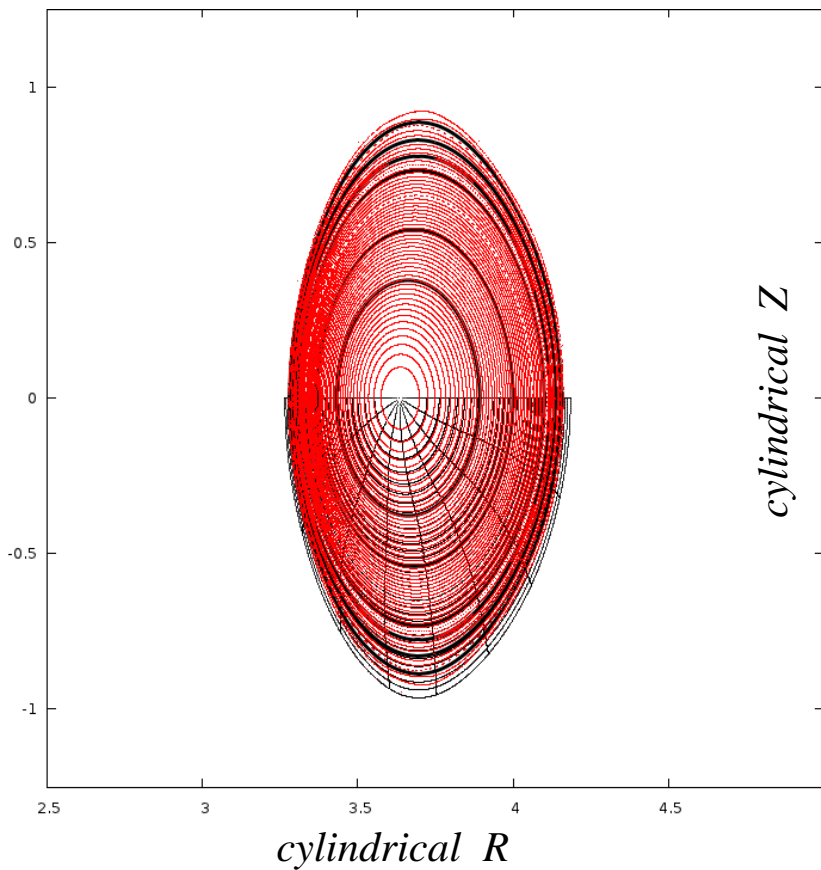


Straight field line coordinates can be constructed over the domain where invariant flux surfaces exist



Near the plasma edge, there are magnetic islands, chaotic field lines.  
Lets take a closer look . . . . .

Now, examine the “edge” . . . .

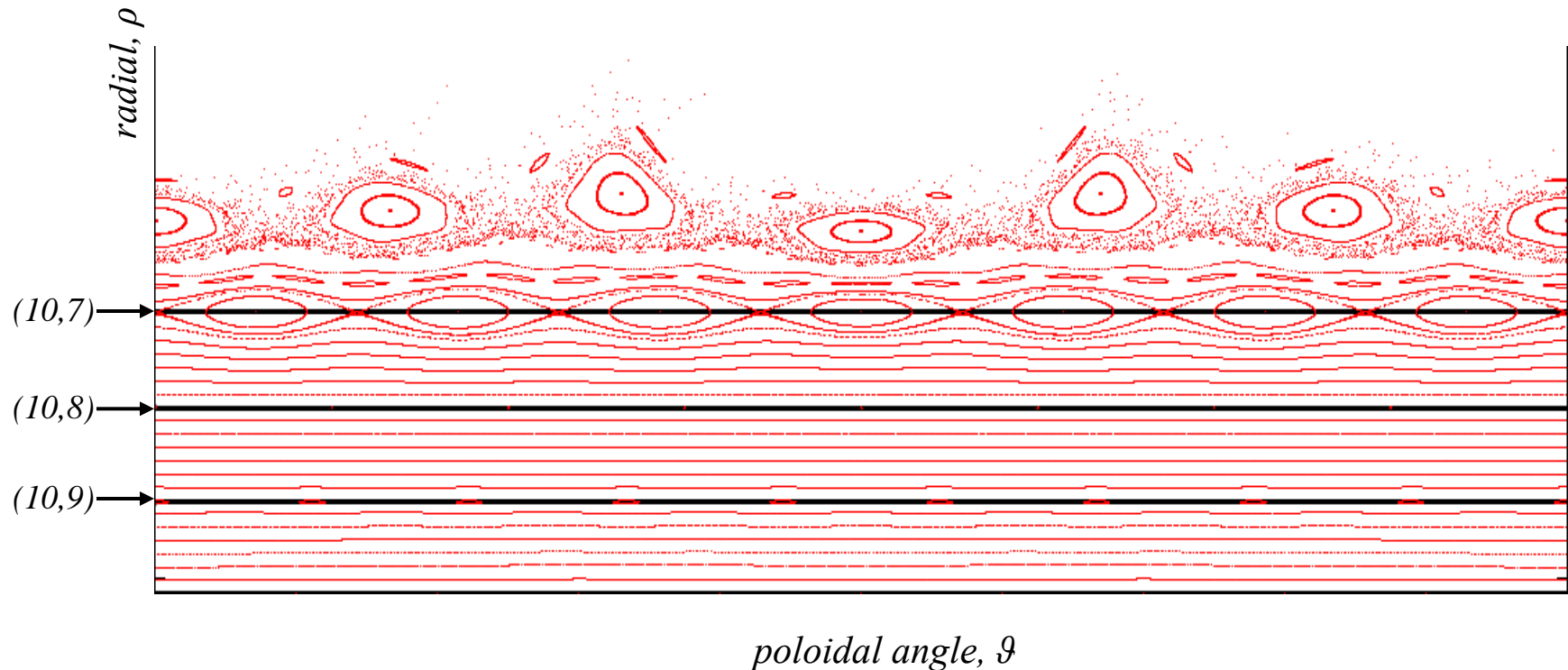


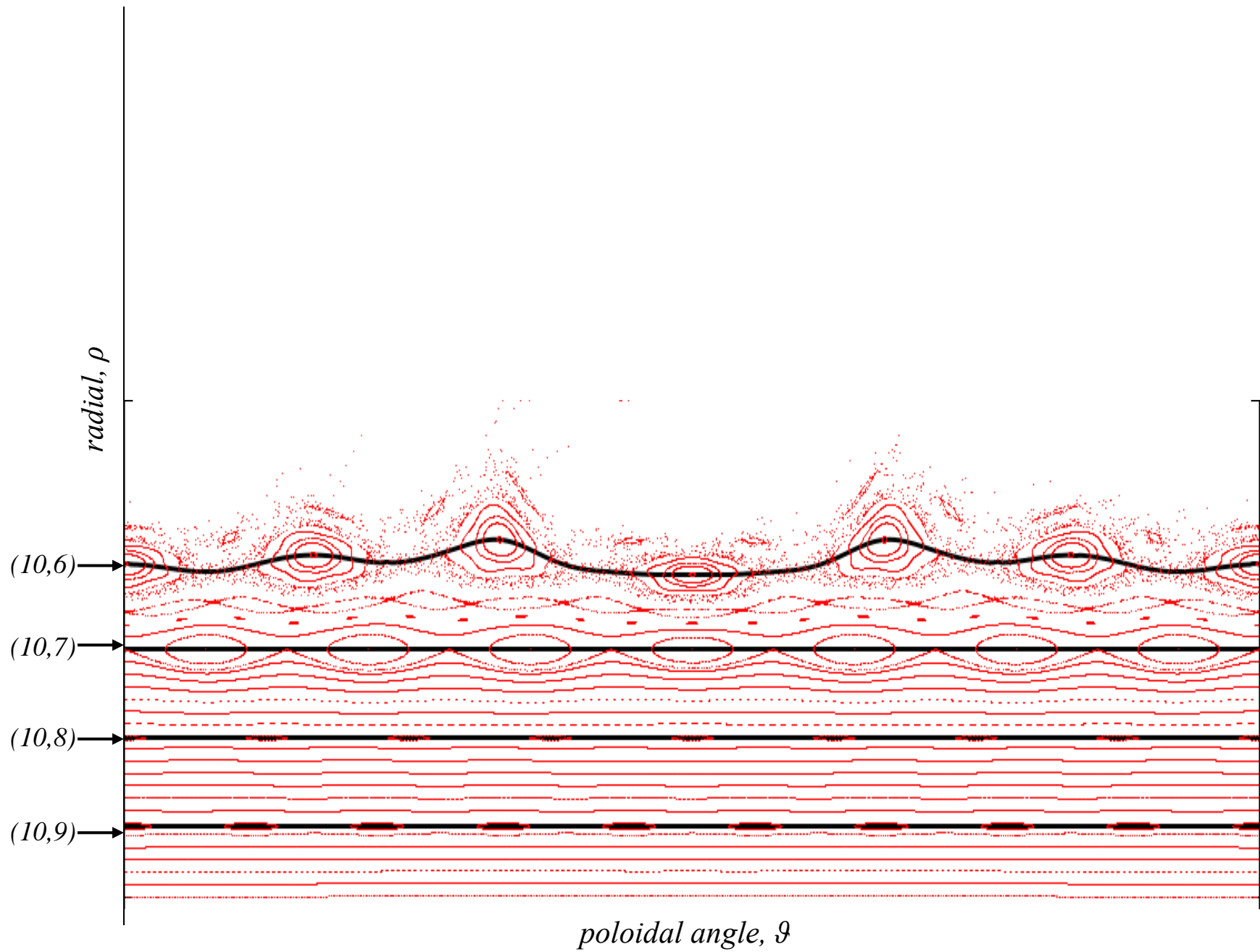
Near the plasma edge,  
there are magnetic islands and field-line chaos

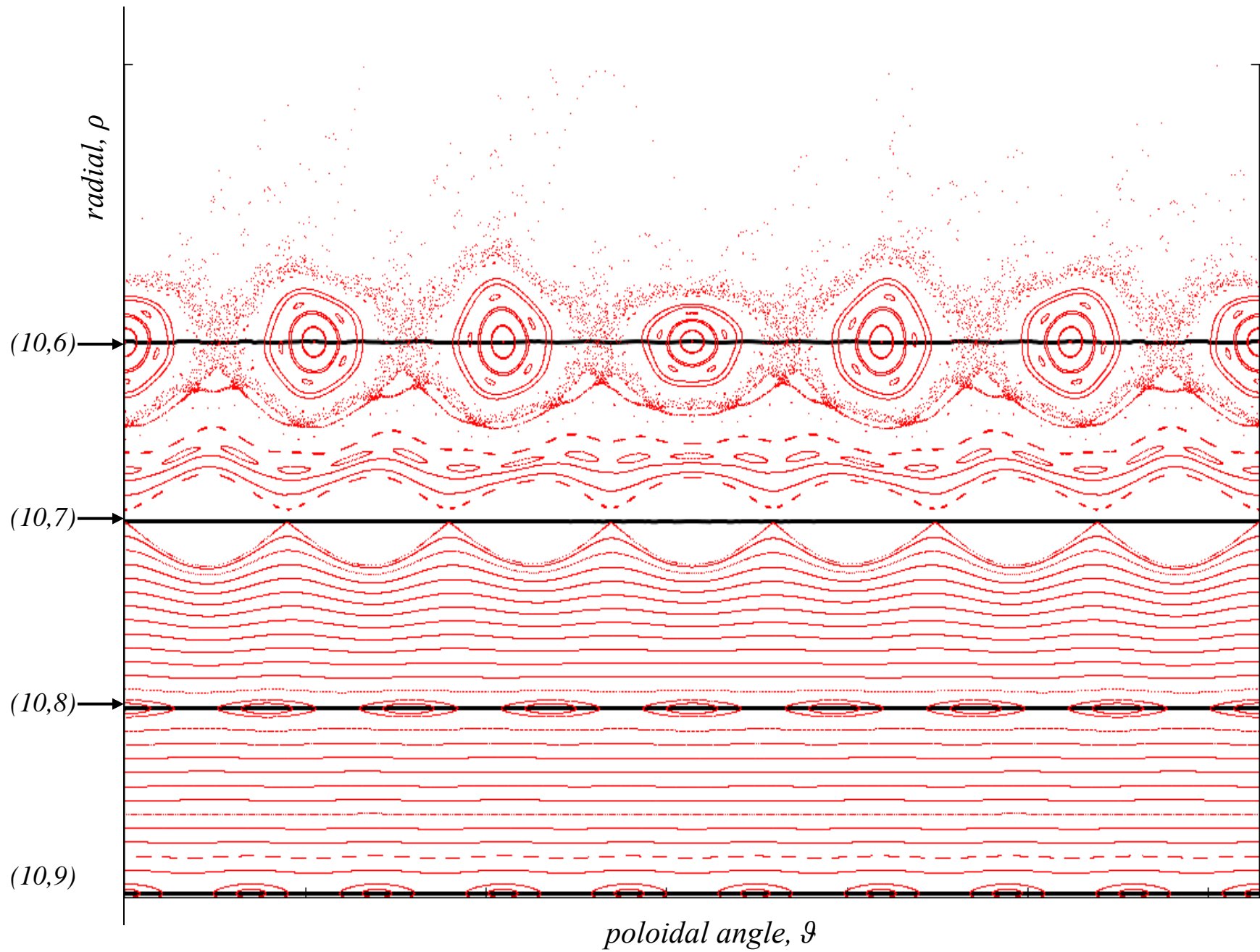
But this is no problem. There is no change to the algorithm!

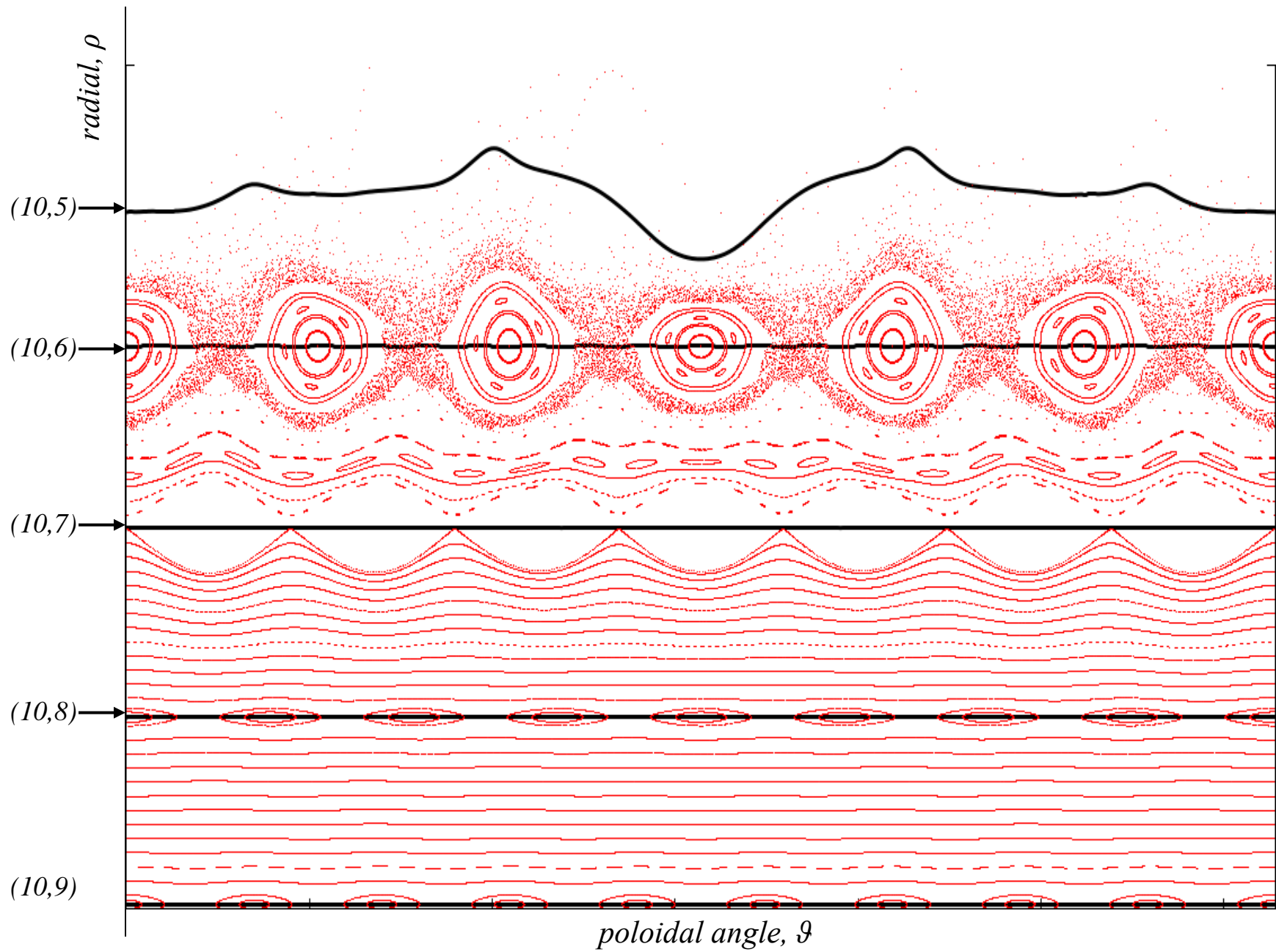
The rational, almost-invariant surfaces can still be constructed.

The quadratic-flux minimizing surfaces  $\approx$  ghost-surfaces pass through the island chains,









# Now, lets look for the ethereal, last closed flux surface.

(from dictionary.reference.com)

e•the•re•al [ih-theer-ee-uhl]

*Adjective*

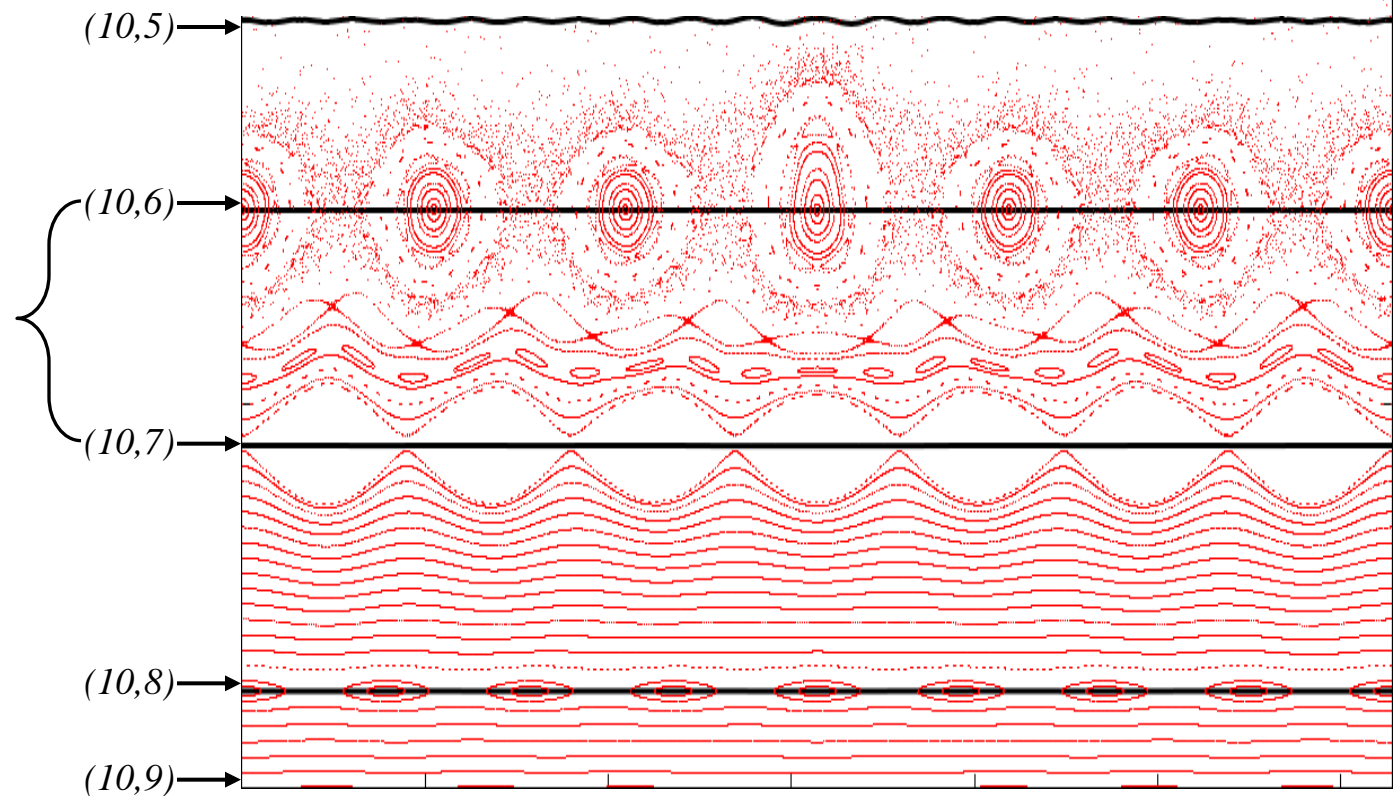
1.light, airy, or **tenuous**: *an ethereal world created through the poetic imagination.*

2.**extremely delicate** or refined: *ethereal beauty.*

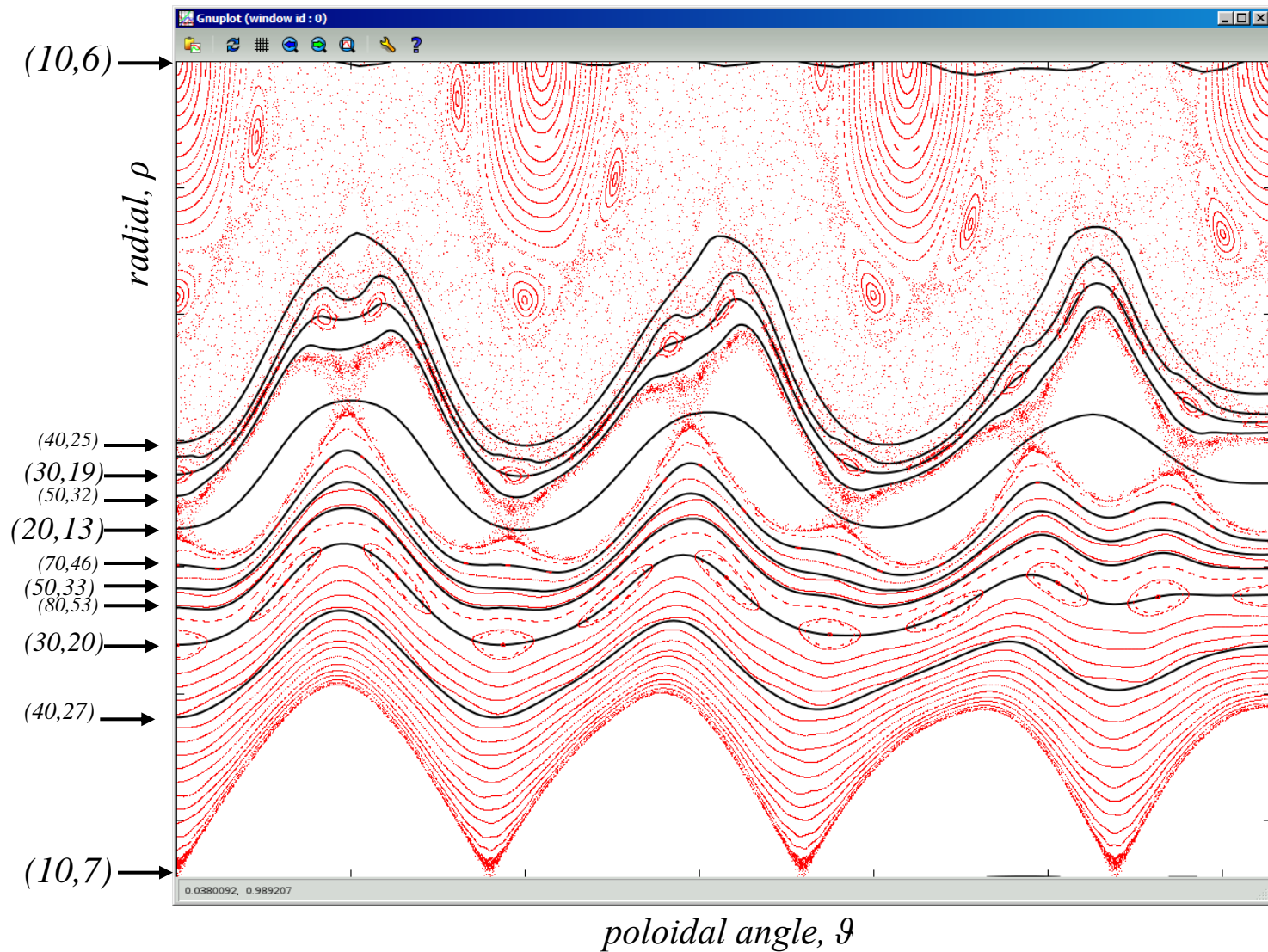
3.heavenly or celestial: *gone to his ethereal home.*

4.of or pertaining to **the upper regions of space.**

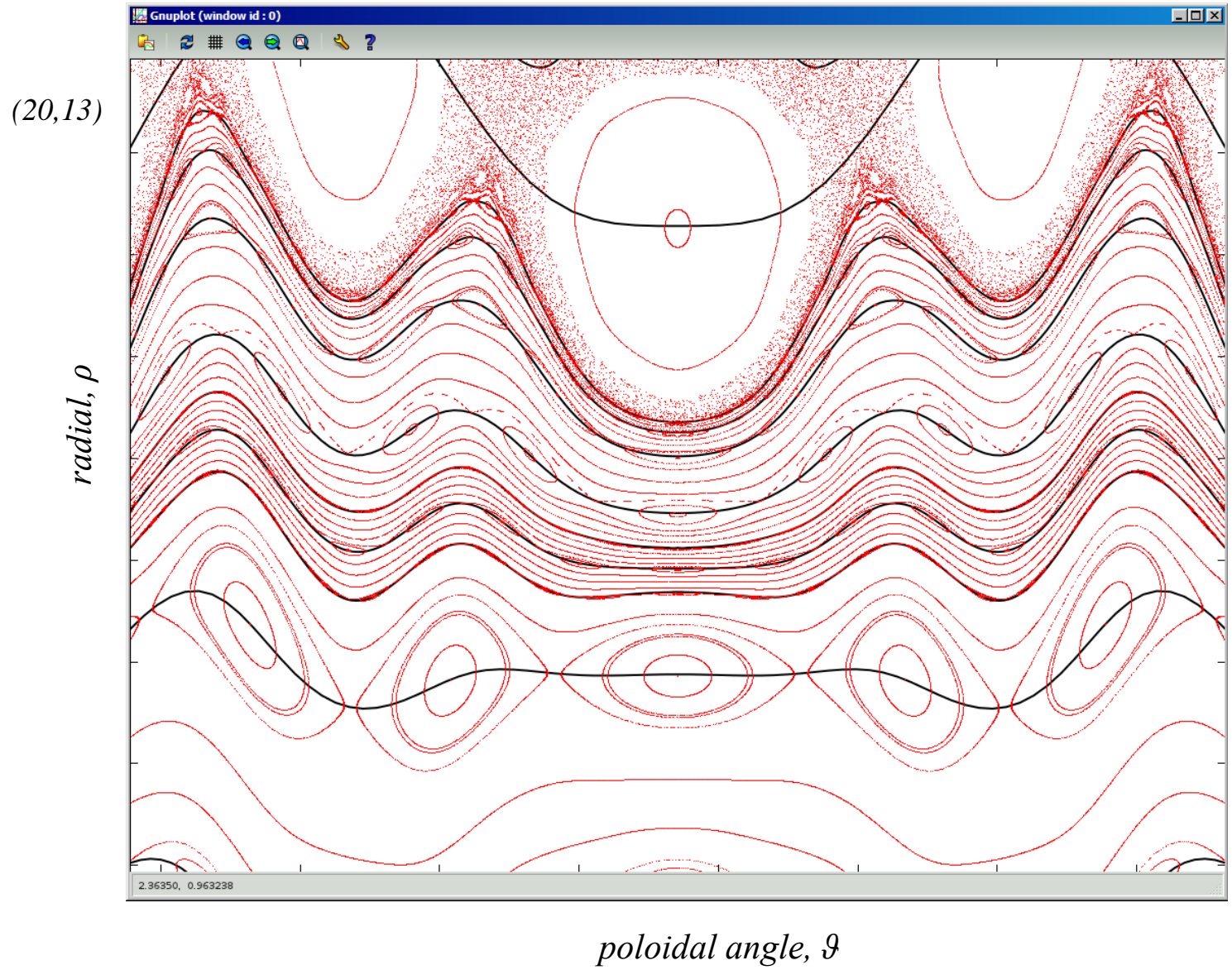
Perhaps the last flux surface is in here

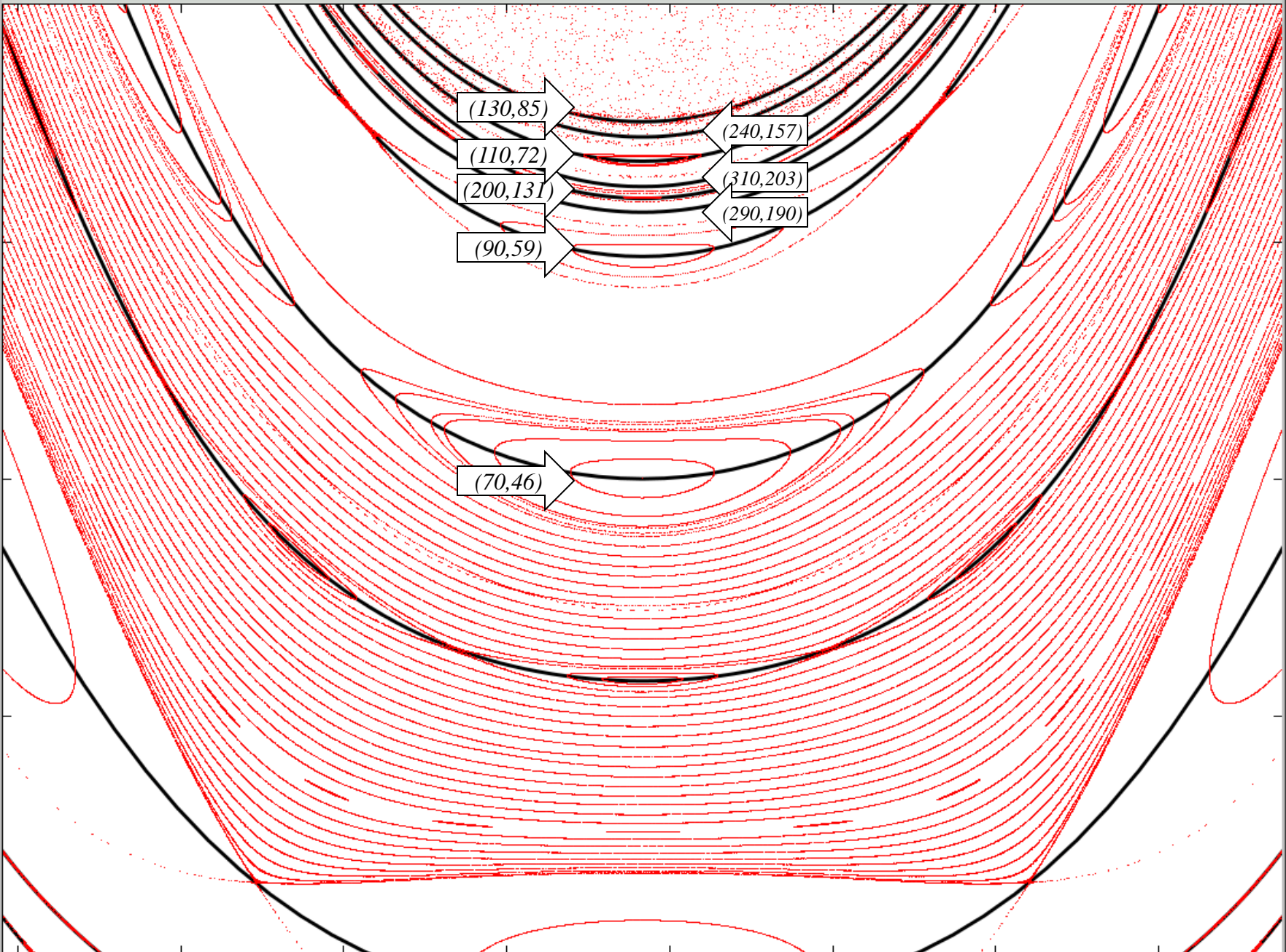




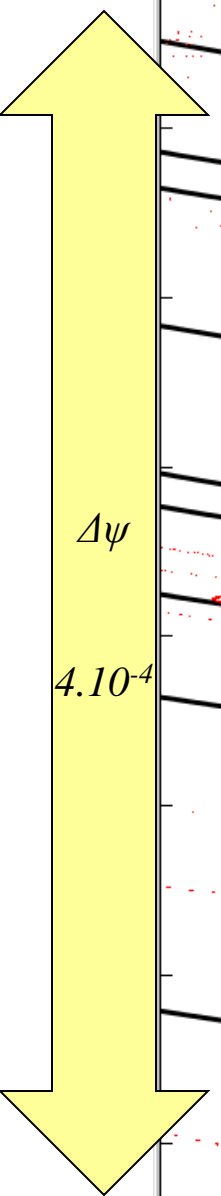


Hereafter, will not Fourier decompose the almost-invariant surfaces and use them as coordinate surfaces. This is because they become quite deformed and can be very close together, and the simple-minded piecewise cubic method fails to provide interpolated coordinate surfaces that do not intersect.





$\rho=0.962810$



(130,85)

(350,229)

(240,157)

locally most noble  $(110\gamma+350)/(72\gamma+29) = 1.5281797735\dots$

(110,72)

locally most noble  $(110\gamma+420)/(72\gamma+275) = 1.5274230155\dots$

(420,275)

(310,203)

(200,131)

(290,190)

(90,59)

$\mathcal{G}=3.11705$

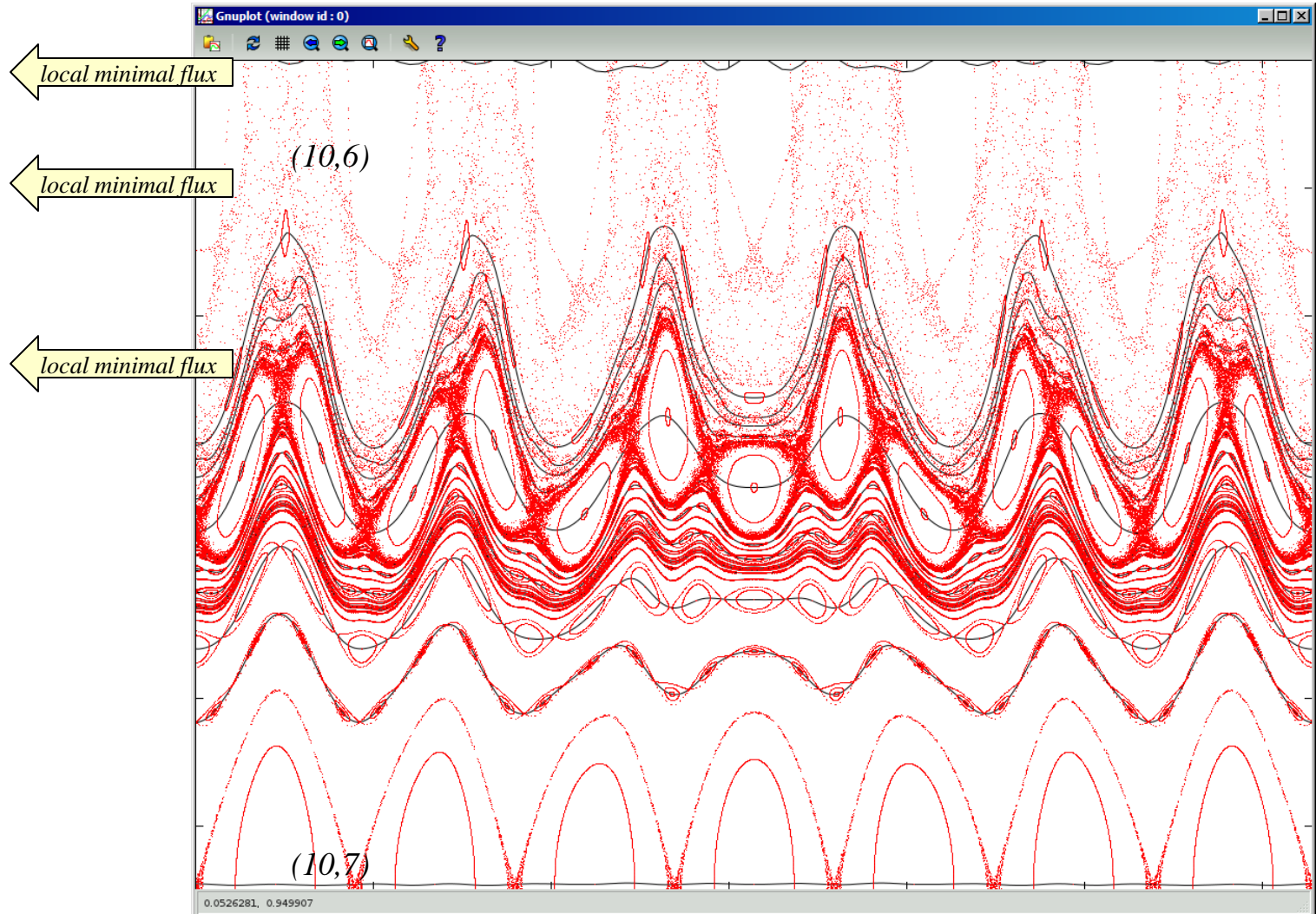
$\mathcal{G}=3.16614$

$\rho=0.962425$

0.962639

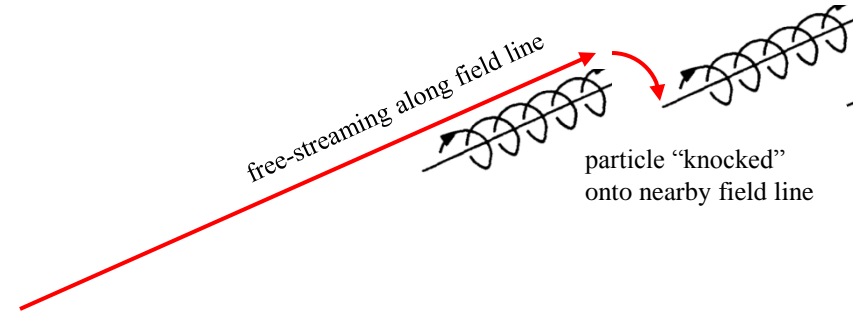
To find the significant barriers to field line transport, construct a hierarchy of high-order surfaces, and compute the upward flux

$\Psi_{10/7}$	$7.50156 \times 10^{-04}$
$\Psi_{40/27}$	$5.35875 \times 10^{-06}$
$\Psi_{30/20}$	$2.17100 \times 10^{-05}$
$\Psi_{110/73}$	$5.76470 \times 10^{-08}$
$\Psi_{80/53}$	$3.18777 \times 10^{-07}$
$\Psi_{290/192}$	$2.90328 \times 10^{-11}$
$\Psi_{210/139}$	$5.10028 \times 10^{-10}$
$\Psi_{340/225}$	$4.32721 \times 10^{-12}$
$\Psi_{130/86}$	$2.10427 \times 10^{-08}$
$\Psi_{180/119}$	$2.95639 \times 10^{-09}$
$\Psi_{230/152}$	$2.23672 \times 10^{-09}$
$\Psi_{50/33}$	$3.67232 \times 10^{-06}$
$\Psi_{120/79}$	$7.86600 \times 10^{-08}$
$\Psi_{70/46}$	$1.37526 \times 10^{-06}$
$\Psi_{90/59}$	$8.35105 \times 10^{-07}$
$\Psi_{290/190}$	$6.50293 \times 10^{-08}$
$\Psi_{200/131}$	$7.07049 \times 10^{-08}$
$\Psi_{310/203}$	$3.85707 \times 10^{-07}$
$\Psi_{420/275}$	$3.73482 \times 10^{-07}$
$\Psi_{110/72}$	$8.62439 \times 10^{-07}$
$\Psi_{350/229}$	$1.29837 \times 10^{-07}$
$\Psi_{240/157}$	$4.27556 \times 10^{-07}$
$\Psi_{130/85}$	$6.22742 \times 10^{-07}$
$\Psi_{20/13}$	$1.87579 \times 10^{-04}$
$\Psi_{90/58}$	$4.90660 \times 10^{-06}$
$\Psi_{70/45}$	$7.79506 \times 10^{-06}$
$\Psi_{50/32}$	$1.89412 \times 10^{-05}$
$\Psi_{80/51}$	$7.84026 \times 10^{-06}$
$\Psi_{30/19}$	$9.25352 \times 10^{-05}$
$\Psi_{10/6}$	$3.71570 \times 10^{-03}$



# The construction of chaotic coordinates simplifies anisotropic diffusion

$$\frac{\partial T}{\partial t} = \nabla \cdot (\kappa_{\parallel} \nabla_{\parallel} T + \kappa_{\perp} \nabla_{\perp} T) + Q,$$



In chaotic coordinates, the temperature becomes a surface function,  $T=T(s)$ , where  $s$  labels invariant (flux) surfaces or almost-invariant surfaces.

If  $T=T(s)$ , the anisotropic diffusion equation can be solved analytically,  $\frac{dT}{ds} = \frac{c}{\kappa_{\parallel} \varphi + \kappa_{\perp} G}$ ,

where  $c$  is a constant, and

$\varphi = \int \int d\theta d\phi \sqrt{g} B_n^2$ , is related to the quadratic-flux across an invariant or almost-invariant surface,

$G = \int \int d\theta d\phi \sqrt{g} g^{ss}$ , is a geometric coefficient.

**An expression for the temperature gradient in chaotic fields**

S.R. Hudson, Physics of Plasmas, 16:010701, 2009

**Temperature contours and ghost-surfaces for chaotic magnetic fields**

S.R.Hudson and J.Breslau

Physical Review Letters, 100:095001, 2008

When the upward-flux is sufficiently small, so that the parallel diffusion across an almost-invariant surface is comparable to the perpendicular diffusion, the plasma cannot distinguish between a perfect invariant surface and an almost invariant surface

# Comments

- 1) Constructing almost-invariant surfaces is very fast, about 0.1sec each surface, and each surface may be constructed in parallel. (In fact, each periodic curve on each surface can be constructed in parallel.)
- 2) To a very good approximation, the pressure becomes a surface function,  $p=p(\rho)$ , (where the pressure, temperature satisfy an anisotropic diffusion equation)
- 3) Chaotic-coordinates are straight-field line coordinates on the periodic orbits (and the KAM surfaces), and

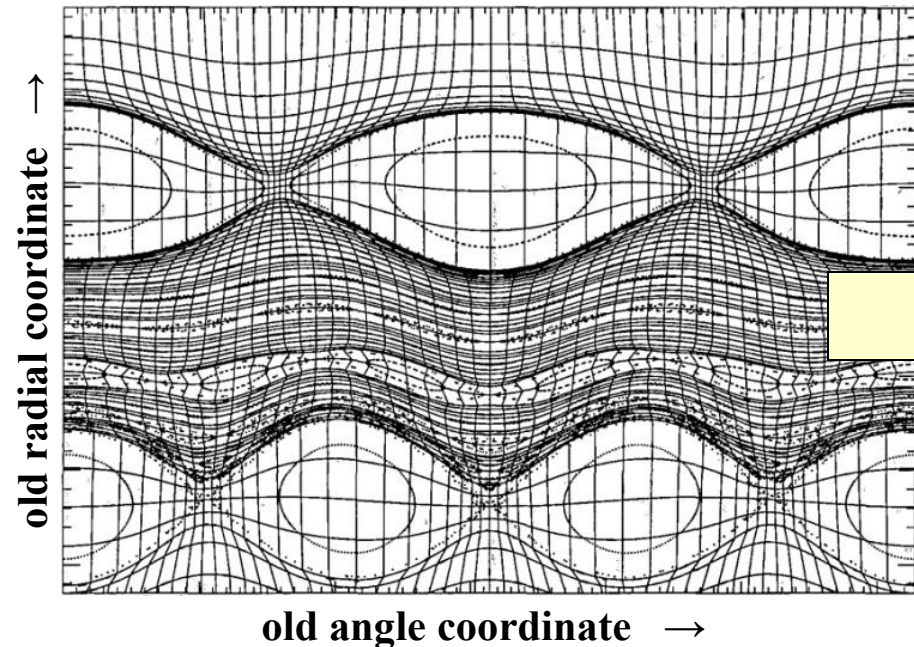
are *nearly* straight field line coordinates throughout the domain ( $\vartheta$  is linear,  $\psi$  is constant).

$$Eqn(1) \quad \mathbf{A} = \psi \nabla \theta - \chi(\psi, \theta, \zeta) \nabla \zeta \quad \chi(\psi, \theta, \zeta) = \chi_0(\psi) + \epsilon \chi_1(\psi, \theta, \zeta) \quad \begin{array}{l} \dot{\theta} \approx \chi'_0(\psi) \\ \dot{\psi} \approx 0 \end{array}$$

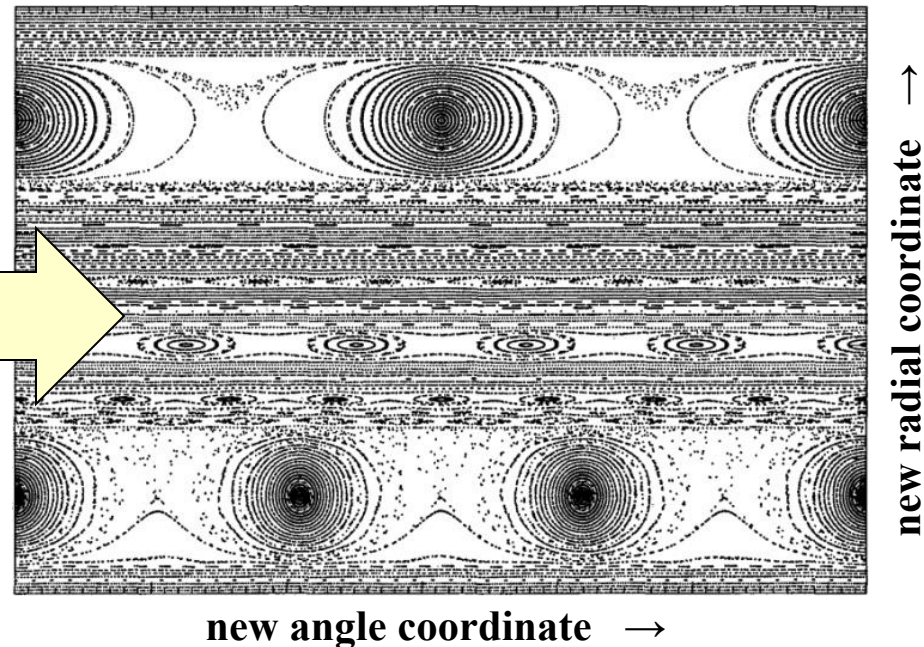
- 1) The last closed flux surface can be determined using a systematic, reliable method, and the upward magnetic-field line flux across near-critical cantori near the plasma edge can be determined. There is not one “plasma boundary”. Depending on the physics, there is a hierarchy of “partial boundaries”, which coincide with the surfaces of locally minimal flux.
- 2) Chirikov island overlap estimate is easily estimated from Eqn(1) above, and Greene’s residue criterion is easily calculated by the determinant of the Hessian.

# Chaotic coordinates “straighten out” chaos

Poincaré plot of chaotic field  
(in **action-angle** coordinates of **unperturbed** field)



Poincaré plot of chaotic field  
in **chaotic** coordinates



phase-space is partitioned into (1) **regular (“irrational”) regions**  
and (2) **irregular (“rational”) regions**

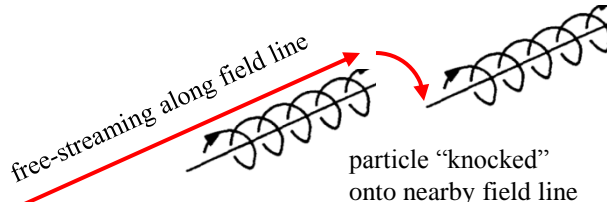
with “good flux surfaces”, temperature gradients  
with islands and chaos, flat profiles



# Chaotic coordinates simplify anisotropic transport

## The temperature is constant on ghost surfaces, $T=T(s)$

1. Transport *along* the magnetic field is *unrestricted*  
 → consider parallel random walk, with **long** steps  $\approx$  collisional mean free path
2. Transport *across* the magnetic field is *very small*  
 → consider perpendicular random walk with **short** steps  $\approx$  Larmor radius



3. Anisotropic diffusion balance

$$\kappa_{\parallel} \nabla_{\parallel}^2 T + \kappa_{\perp} \nabla_{\perp}^2 T = 0, \quad \kappa_{\parallel} \gg \kappa_{\perp}, \quad \kappa_{\perp} / \kappa_{\parallel} \sim 10^{-10}$$

$2^{12} \times 2^{12} = 4096 \times 4096$  grid points  
(to resolve small structures)

4. Compare solution of numerical calculation to ghost-surfaces

5. The temperature adapts to KAM surfaces, cantori, and ghost-surfaces!

*i.e.*  $T=T(s)$ , where  $s=const.$  is a ghost-surface

from  $T=T(s, \theta, \phi)$  to  $T=T(s)$  is a fantastic simplification, allows analytic solution

$$\frac{dT}{ds} \propto \frac{1}{\kappa_{\parallel} \phi_2 + \kappa_{\perp} G}$$

**Temperature contours and ghost-surfaces for chaotic magnetic fields**  
 S.R. Hudson et al., Physical Review Letters, 100:095001, 2008  
 Invited talk 22<sup>nd</sup> IAEA Fusion Energy Conference, 2008  
 Invited talk 17th International Stellarator, Heliotron Workshop, 2009

**An expression for the temperature gradient in chaotic fields**  
 S.R. Hudson, Physics of Plasmas, 16:100701, 2009

